

Methods for Gait Analysis in a Supportive Smart Home

by

Ashi Agarwal, B.Tech.

A thesis submitted to the Faculty of Graduate and Postdoctoral
Affairs in partial fulfillment of the requirements for the degree of

Master of Applied Science

in

Electrical and Computer Engineering

Carleton University
Ottawa, Ontario

© 2022, Ashi Agarwal

Abstract

According to study, the elderly's mobility habits are closely tied to cognitive decline and other age-related health problems. Regular gait analysis may help with the early detection of various disorders, but the gathering of daily ambient data is difficult with current technology. The potential of ambient sensors on the market for estimating gait speed is examined in this thesis. The thesis's first section analyses data gathered from four motion sensors that were arranged in a straight line on the ceiling as used in some wide scale studies. The findings of this work indicate that the communications protocol limits the accuracy of gait speed estimation, which prompted the investigation of AI-enabled privacy-respecting cameras. Initial results showed the camera performance was limited by low and asynchronous frame rate, which led to significant error margins. A method is proposed that reduces this to 6% using techniques based on regression and interpolation.

Acknowledgements

At first, I would like to extend my sincerest gratitude to my academic supervisors, Dr. Rafik Goubran and Dr. Bruce Wallace, for their support and guidance that I received throughout the progress of my thesis. I've been fortunate enough to have two supervisors who were able to successfully lead me through this process, as well as two mentors who have pushed me to pursue goals beyond my limits. I also want to thank my medical advisors, Dr. Frank Knoefel and Dr. Neil Thomas, for their guidance on all clinical matters and for always making time in their busy schedules to provide insight on all the written material I sent to them.

I would like to thank Laura Ault for helping me set up a mini-lab in my home amid COVID and Julien Larivière-Chartier for assisting me with all the complicated programming and technology that I was unfamiliar with. Thanks are also due to Jeffrey Kaye, Zachary Beattie and the whole CART team for providing me with the data to work on.

Additionally, I would like to heartily thank my family for always being there for me while being miles apart and loving me unconditionally. Last but not the least, thanks are due to all my friends who helped me adjust to a new country and supported me in all highs and lows and even agreed to be monitored in their own house for my data collection process.

Table of Contents

Abstract.....	ii
Acknowledgements	iii
Table of Contents	iv
List of Tables	vii
List of Figures.....	viii
List of Acronyms	x
Chapter 1: Introduction	1
1.1 Motivation	1
1.2 Problem Statement.....	2
1.3 Objective.....	3
1.4 Summary of Contributions	3
1.4.1 Collaborators	5
1.5 Thesis Structure	6
Chapter 2: Background.....	8
2.1 Introduction	8
2.2 Importance of Gait Analysis.....	8
2.3 Clinical Methods of Cognitive Analysis	10
2.3.1 Gait Analysis and Cognition Decline.....	13
2.4 Clinical Methods of Gait Analysis	14
2.5 Automated Sensors based Gait Assessment	16
2.5.1 Obtrusive Gait Assessment	17
2.5.2 Unobtrusive Gait Assessment	18
2.5.2.1 Sound Based Sensors.....	19
2.5.2.2 Light Based Sensors	20

2.5.2.3	Force Sensors	22
2.6	Summary.....	23
Chapter 3: Evaluating changes in Gait and Activity Associated with Cognitive Impairment..... 25		
3.1	Introduction	25
3.1	Gait Line.....	25
3.1.1	Sensor Deployment	26
3.1.2	Data Acquisition.....	27
3.2	Preliminary Data Analysis.....	28
3.2.1	Data Cleaning.....	28
3.2.2	Observations on Cleaned Data	29
3.3	Identification of Walks	30
3.4	Results	34
3.5	Conclusion.....	35
Chapter 4: Using Zigbee Sensors for Ambient Measurement of Human Gait – Analytical Considerations 36		
4.1	Experimental Setup	36
4.2	Ottawa Residences’ Data Analysis.....	37
4.2.1	Observation and Discussion.....	38
4.3	Controlled Experiment Data Analysis.....	42
4.4	Zigbee Protocol Analysis	43
4.4.1	Intro to Zigbee Protocol	44
4.4.2	Delay Calculation.....	48
4.5	Conclusion.....	50
Chapter 5: Walking Gait Speed Measurement Using Privacy Respecting AI Enabled Visual Sensor 51		

5.1	AltumView Sentinare Activity Visual Sensor.....	51
5.1.1	Experiment Setup.....	52
5.1.2	Data Acquisition.....	55
5.1.3	Verification	56
5.2	Methodology.....	57
5.2.1	Sensor Calibration.....	58
5.2.2	Relative Location Estimation	59
5.2.3	Gait Estimation.....	60
5.3	Results	61
5.4	Discussion.....	62
Chapter 6: Method to Improve Gait Speed Assessment for Low Frame Rate AI Enabled Visual Sensor		65
6.1	Methodology.....	65
6.1.1	Walk Data Overview.....	66
6.1.2	Peak and Valley Location	67
6.1.3	Curve Fitting and Data Estimation.....	68
6.1.4	Gait Speed Estimation.....	69
6.2	Results	70
6.3	Discussion.....	74
Chapter 7: Conclusion and Future Work.....		75
7.1	Thesis Conclusion	75
7.2	Thesis Contribution	78
7.3	Thesis Limitations	78
7.4	Future Work.....	79
References		81

List of Tables

Table 4.1 Total time recorded by both set of sensors and their difference © 2021 IEEE	43
Table 4.2 Delay Estimates induced by both CSMA/CA technique based on number of back off(s) © 2021 IEEE	49
Table 5.1 Average Error in Gait Speed © 2022 IEEE	61
Table 5.2 Difference in IR and Cam Time Stamps © 2022 IEEE	63
Table 6.1 Root Mean Square Error (in pixels) © 2022 IEEE	70
Table 6.2 Average error of gait speed estimation © 2022 IEEE	73

List of Figures

Figure 3.1 Illustration of Gait Line and section definition	27
Figure 3.2 Screenshot of pre-processed data (a) Missing sensor event (b) Out of order event.....	29
Figure 3.3 Screenshot illustration of window and its movement.....	31
Figure 3.4 Number of walks per week according to all 6 definitions for a sample home	33
Figure 3.5 Average number of walks per hour over a day.....	34
Figure 3.6 Average number of walks per week over a 3-month period	35
Figure 4.1 Screenshot of pre-processed data (a), (b) Classified as non-walks (c) Classified as walk © 2021 IEEE.....	38
Figure 4.2 Histogram of time intervals for House 1 in direction (a)1 to 4 (b) 4 to 1 © 2021 IEEE.....	40
Figure 4.3 Scatter plot of time intervals in direction 4 to 1 for House 1 © 2021 IEEE ...	40
Figure 4.4 House layout map for the sample house in conversation	41
Figure 4.5 Example of superframe structure sourced from IEEE Std. 802.15-4 Figure 6-1 © 2020 IEEE.....	45
Figure 4.6 Flow Chart depicting process any sensor undergoes while transmitting a message to the hub	46
Figure 5.1 (a) Lab setup (b) AltumView Sensor view of Lab setup with a sample stick figure © 2022 IEEE	53
Figure 5.2 Illustration of lab setup (a) Side View (b) Top View © 2022 IEEE	54
Figure 5.3 Illustration comparing field of view of camera at different heights © 2022 IEEE.....	54

Figure 5.4 Flow Chart Explaining methodology	57
Figure 5.5 (a) Background Image with calibrated markers (b) Binary image created after calibration © 2022 IEEE.....	58
Figure 5.6 Diagram representing Relative location estimation © 2022 IEEE.....	60
Figure 5.7 Screenshot of the processed data (1) Time stamp (2) Frame number (3) Person ID (4) Right Ankle coordinates (5) Left Ankle coordinates (6) All body coordinates © 2022 IEEE	62
Figure 6.1 Graph of x-y coordinates of both ankles versus the frame number.....	67
Figure 6.2 Graph representing the estimated y coordinates versus frame data for both ankles, by all three regressed polynomials. The region shown in the black box is enlarged in Figure 6.3 © 2022 IEEE.	72
Figure 6.3 Example enlargement showing the difference between the regression curves for the quadratic, cubic and linear polynomial when the subject ankles are close the camera. This is an enlargement of the region shown in Figure 6.2 © 2022 IEEE.....	73

List of Acronyms

2D	2-Dimensional
3D	3-Dimensional
AD	Alzheimer's' Disease
AI	Artificial Intelligence
BE	Back off Exponent
BI	Beacon Interval
BLE	Battery Life Extension
CAP	Contention Access Period
CART	Collaborative Aging Research using Technology
CCA	Clear Channel Assessment
CDR	Clinical Dementia Rating
CFP	Contention Free Period
CNN	Convolutional Neural Network
CP	CANDECOMP/PARAFAC decomposition
CSI	Channel State Information
CSMA/CA	Carrier Sense Multiple Access with Collision Avoidance
CSV	Comma-Separated Values

EMG	Electromyography
GRF	Ground Reaction Force
GTS	Guaranteed Time Slot
HC	Healthy Control
IFS	Intraframe Spacing
IR	Infra Red
ITG	Infrared Thermography
MoCA	The Montreal Cognitive assessment
MCI	Mild Cognitive Impairment
PAN	Personal Area Network
PC	Personal Computer
PVC	Polyvinyl Chloride
RGB	Red-Green-Blue
RGBD	Red-Green-Blue-Depth
SD	Superframe Duration
ToF	Time of Flight

Chapter 1: Introduction

This chapter details the motivation for this thesis, reviews the problem statement and objectives as well as states contributions of the thesis and contributions made by each collaborator, while ending with the description of the thesis structure.

1.1 Motivation

Statistics Canada reported in 2019 that the estimated number of senior citizens added up to 17.5% of the overall Canadian population, while the percentage of children in the age bracket of 0 to 14 years only adds up to 16% indicating that the number of senior citizens has far exceeded the number of younger generation [1]. In 2011, Statistics Canada reported that the growth rate for people 65 and older (14.1%) exceeded that of children under the age of 14 (0.5%) and those aged 15 to 64 (5.7%). These figures reflect the rapidly aging Canadian population. This demographic shift will shape our society over the next 20 to 30 years is expected to have a profound impact on individuals, communities, and health services. Imminent demographic change is a well-known phenomenon; National strategies have been developed to help prepare Canada for the challenges it presents [2]. Caring for Canada's aging population and the global population in general is one of the most pressing issues that can have serious implications for the health care system and economy. That's why policy makers across the country and around the world are encouraging aging at home. In addition to making the country's healthcare system more resilient, it allows older people to be closer to loved ones and spend time in the neighborhood, keeping them active and fit [3]. Despite the advice of policymakers and the preferences of older people, aging has its own set of challenges. The unpaid work provided by caregivers to make aging possible

often places a burden on them, affecting their health [4], [5]. Tired caregivers not only end up with reduced work efficiency, but additional negative consequences on their own well-being. However, the recent advancements in the technology and practicality of the smart homes have provided hopes for automated health monitoring and assessment, easing the burden of caregivers [6], [7]. This work aims to not only maintain but improve the quality of aging care provided by harnessing the innate ability of technology to capture the human activities without interfering with them.

1.2 Problem Statement

Mobility impairments have always been one of the most prominent health indicators in geriatric care often indicating frailty [8]. The senescent population have a complex relationship with mobility and its decline could often be an indicator of their declining health caused by various underlying diseases [9]. Therefore gait analysis becomes a crucial measure among required regular health checkups for the elderly [10].

The rapidly aging population of Canada needs more and more attention from the medical care system of the country, a system which was not initially designed to meet the challenges put forth by aging population. In addition, population aging is generally one of the driving factors of increasing health care costs as health care costs per individual increases with age [11]. Thence as mentioned earlier, elderly care in Canada poses major impacts over the health care system and economy of the country, raising serious concerns for the policy makers which can be helped by adapting to technology based monitoring for elderly at the comfort of their homes [12].

Considering the importance of regular gait monitoring at the same time and shortcomings of health care system to meet the requirements of aging population of Canada; a precise technology based solution could provide major assistance to the issue.

1.3 Objective

The main objective of this work is to evaluate the feasibility of current smart home technologies and their ability to accurately assess the walking speed of its residents. This work also extends to suggest better alternatives to the existing sensor networks. The algorithms developed during this thesis are primarily designed to determine the time required to walk a pre-known distance, and thus calculating the walking speed. A series of increasingly complex experiments were designed and conducted, where each experiment is trying to improve and resolve the limitations identified by the previous one thus continuously improving the end results.

1.4 Summary of Contributions

This thesis was built upon several stages of research. The contributions presented in this section are representative of these stages and include:

1. The first step was to establish the relationship between the mobility and cognitive abilities of the older generation highlighting the importance of gait assessment. This was achieved by analyzing over 90 days of data from 32 single resident households across USA for subjects from the Collaborative Aging Research using Technology (CART) network. Two groups of subjects with and without cognitive decline were analyzed which is the first contribution of this thesis. The beforementioned work was published in a medical conference in form of following poster [13].

- Neil Thomas, Ashi Agarwal, Laura Ault, Julien Laviere Chartier, Bruce Wallace, Rafik Goubran, Frank Knoefel, Zachary Beattie, Jefferey Kaye, “Evaluating changes in gait and activity associated with cognitive impairment using a home-based technology platform,” *Alzheimer’s Association International Conference*.
2. After establishing the importance of gait assessment, the next was to calculate the gait speed with the help of existing data collected from the CART network. During the analysis, it was discovered that sensors which communicate through battery saving protocols like Zigbee [96] have limitations when used. They may not be suitable for time sensitive measurements like gait speed as they introduce unavoidable random amounts of delay during transmission which contributed to the second major contribution of this thesis. The results from this experiment and added analysis performed to confirm the theory are all detailed in Chapter 5. This work was published in following paper [14].
- Ashi Agarwal, Bruce Wallace, Laura Ault, Julien Laviere Chartier, Frank Knoefel, Rafik Goubran, Jefferey Kaye, Zachary Beattie, Neil Thomas, “Using Zigbee Sensors for Ambient Measurement of Human Gait – Analytical Considerations,” *2021 IEEE International Symposium on Medical Measurements and Applications (MeMeA)*
3. As the second contribution suggested, there was a need for better alternatives for gait assessment, hence an algorithm was designed to calculate gait speed from a novel privacy respecting AI enabled camera which is the third contribution of this thesis. The experimental results established the potential of the visual sensor whilst

pointing out some major concerns over asynchronous and low frame rate of the visual sensor, the algorithms and experimental results are all explained in Chapter 6. This work was published in a conference in the form of following paper [15].

- Ashi Agarwal, Bruce Wallace, Rafik Goubran, Frank Knoefel, Neil Thomas, “Walking Gait Speed Measurement Using Privacy Respecting AI Enabled Visual Sensor,” *IEEE 2022 International Symposium on Medical Measurements and Applications (MeMeA)*.

4. As the previous results suggested, low and asynchronous frame rate posed major concerns over the precision of gait speed estimation. It was addressed by designing a regression-based algorithm to restore the frame rate to the original frame rate of 30 frames/sec which makes up the fourth contribution of this thesis. The algorithm compares results from regression of three different degrees of freedom, the experimental results and concluding discussion are all explained in chapter 7. This work was submitted and accepted in *Sensors Application Symposium 2022* [16].

- Ashi Agarwal, Bruce Wallace, Rafik Goubran, Frank Knoefel, Neil Thomas, “Method to Improve Gait Speed Assessment for Low Frame Rate AI Enabled Visual Sensor,” *IEEE 2022 Sensors Application Symposium (SAS)*.

1.4.1 Collaborators

- Bruce Wallace: Thesis Supervisor
- Rafik Goubran: Thesis Supervisor

- Frank Knoefel: Medical doctor and researching physician with extensive expertise in aging and geriatric care.
- Neil Thomas: Medical Expert and a researching physician with a practice in Dementia care, completed a residency at OHSU where CART project is based. First author in the medical paper where he presented the idea and contributed by drawing observations on experiment results and cognitive test scores of participants.
- Julien Laviere Chartier: Tech support, fetched data from CART servers and designed code to convert it to MATLAB structures.
- Laura Ault: Helped with installation of CART sensors in houses in Ottawa.
- Jefferey Kaye: Physician and PI lead for CART
- Zachary Beattie: Engineer at Oregon Health & Science University (OHSU) and technical prime for CART

1.5 Thesis Structure

There are seven chapters in this thesis. The necessity of gait analysis for the early detection of cognitive impairment, the clinical approaches available for gait analysis, and the need for technology-based ambient gait monitoring are all covered in great length in Chapter 2. It goes into further detail on some of the current technology and their drawbacks which provides the background of this thesis. An explanation of a big data analysis experiment employing ceiling-mounted motion sensors to determine the association between cognitive decline and movement patterns in older persons is then provided in Chapter 3. In Chapter 4, a subset of that data and another controlled experiment were used to further examine

anomalies discovered by the observations made in Chapter 3. Chapter 5 and 6 explains two methodologies, their results, and how one was designed on top of the other to overcome hardware limitations, allowing us to use a novel AI enabled privacy respecting camera for gait speed estimation. Chapter 7 offers conclusions from this thesis, touches upon the limitations of this thesis and suggests many potential areas for further research.

Chapter 2: Background

This chapter details background information needed to fully understand the motives behind this thesis project and the previous work upon which this project is built.

2.1 Introduction

In the next few sections, we will provide an overview of the background information surrounding this thesis topic. Typical presentations of disease in older adults, frailty, mobility, and illness are discussed in sections 2.2 and 2.3, as well as the importance and clinical measures of gait assessment. During sections 2.4 and 2.5, we review some of the existing gait assessment methods including both wearable and non-wearable sensors, while pointing out their shortcomings which forms the basis of this thesis where we are offering suggestions for improvement.

2.2 Importance of Gait Analysis

This type of analysis was first studied in the 19th century [17], [18], and its goal has been to quantify and objectively measure the different parameters that characterize gait, so that they can be used in a variety of different applications. A consistent gait monitoring and assessment can help reveal key information on any person's quality of life [19], [20]. The study is of particular interest when trying to track the evolution of different diseases such as cognitive decline [21] and neurological diseases like Parkinson's or multiple sclerosis [22], [23]; stroke-induced changes in ambulation dynamics [24]; and diseases caused by the aging process [25], which in reference to Canada, affects a large percentage of the population. It is crucial that early diagnoses and treatments be found for diseases and their

complications by having accurate, reliable knowledge of gait characteristics at any given time, and monitoring and evaluating them over time [28].

Disease symptoms in older adults, especially people suffering frailty, require keen observation as they can easily be confused for simple aging symptoms [26]. While certain modest cognitive changes are thought to be a normal component of aging, dementia is not. The main effects of typical aging-related declines affecting mental capacity and attention are mild. The loss of other cognitive capacities, such as quick forgetting, trouble navigating, problem-solving, verbal expression, and breaking social norms, may accompany more severe decreases in cognition in atypical aging [27]. The changes in motor system such as excessive tripping, falls, or tremor are also indications of abnormal aging [28]. According to an article [29] published by Weil Institute of Neurosciences, some of the common symptoms to look out for include: getting lost in well-known locations, repeatedly asking questions, strange or inappropriate actions, ignorance of recent events, falls or loss of equilibrium repeatedly, behavioral shifts etc.

The most common unusual health decline symptoms in elderly are known as the “geriatric giants” and are inclusive of: immobility, instability, incontinence, impaired intellect or memory, social isolation and loneliness etc. [30]. The former especially is usually seen as an inevitable a part of aging, often obscuring its standing as a sign of acute unhealthiness. As a result, many people overlook the latter's status as a sign of acute illness, often seeing it as an inevitable part of aging [31]. Around 20% of very old individuals (88+ years old) walk normally [32], so mobility impairments aren't exclusively related to advancing age. Further studies have identified that elderly individuals with gait disorders suffer from dementia and have reduced survival rates compared to their non-impaired peers, supporting

the theory that declining mobility is a sign of underlying disease [31], [33]. This emphasizes the significance of early detection of these unusual aging symptoms, which will help with the early diagnosis of serious impairments in the elderly. Early detection of these incurable diseases aids in preventing future deterioration, which helps older persons age more comfortably.

Moreover according to Stanford Health Care [34], When a patient is suspected of developing dementia, doctors frequently start their examination by asking them about their past. Questions range from their emotional moods to any observable changes in health despite the fact that persons with dementia frequently are in denial or unaware of how their illness is affecting them [35]. Because they do not want to accept the diagnosis and because Alzheimer's disease and other kinds of dementia might initially resemble normal aging, family members may also dispute the reality of the illness. Therefore, it is essential to create technology that can recognize these subtle indications in them.

2.3 Clinical Methods of Cognitive Analysis

Age-related cognitive changes result in different changes in different people. It can be difficult to distinguish between these and the early phases of a dysfunctional condition (disorder); classifications typically hinge on how they affect social, functional, or vocational activities. Based solely on a standard, non-cognitive evaluation, doctors struggle to estimate patients' cognitive function [36], [37]. Cognitive evaluation is an important clinical ability. It makes brain-related illnesses easier to identify and enables more precise assessments of functional capacity. Additionally, during hospital admissions, cognition helps predict mortality [38]. The following are some common uses of cognitive testing: make a differential diagnosis of the cause, rate the severity of a problem, or track the course

of a disease, cognitive assessment. Numerous tools have been created to help the clinician in this process. These range from quick screening tools that take a few minutes to lengthy formal neuropsychological evaluations; the best option will depend on the amount of time available and the goal of the evaluation. This section will discuss the ways of the more widespread methods that doctors use to assess cognition:

1. The Montreal Cognitive assessment (MoCA) [39]: Levels of cognitive impairment are precisely identified by the Montreal Cognitive Assessment (MoCA). The tests' assessments attempt to determine a person's current cognitive aptitude in the areas of language, visuospatial skills, memory and recall, and abstract thought. It takes about ten minutes to administer the MoCA. A score of more than 25 is regarded as normal, with a maximum achievable score of 30. Any score of 25 or less is seen as a sign of cognitive impairment, which can predict or identify the beginning of dementia in patients.
2. Trail Making Test (TMT) [40]: Many types of brain dysfunction, especially those affecting the frontal lobes, can be detected and diagnosed using the Trail Making Test. High-level cognitive abilities including planning, self-control, memory forming, empathy, and attention are controlled by this area of the brain. The test is divided into two sections: Trails A and Trails B, each with an own set of objectives. The aim for Part A is to draw a line as swiftly as possible from one circle to the next in ascending number order, from 1 to 25. In Part B, the participant must join the circles in ascending sequence while switching back and forth between numbers and letters (1 – A – 2 – B – 3 etc.). The Trail Making Test is graded according to how long it takes to finish.

3. Abbreviated Mental Test (AMT) [41]: A 10-item, quick scale called the Abbreviated Mental Test (AMT) is used to examine for impairments. It was created by choosing 10 questions from the lengthier Mental Test Score that had the highest discriminating value [42]. It has elements that call for healthy short- and long-term memory, focus, and orientation. The typical cutoff point is 8 and indicates a serious cognitive deficiency. It might immediately offer a severity assessment similar to what longer tests would yield. It could be able to distinguish between cognitive changes brought on by the post-operative development of delirium. For senior people, administering it takes about 3 minutes.
4. Six-Item Cognitive Impairment Test (6CIT) [43]: The Short Orientation Memory-Concentration Test is another name for the 6CIT. It asks one memory question, two math questions, and three questions about orientation. When the components are rated, they are given a weighting that produces a value between 0 and 28, with higher values signifying more severe cognitive impairment. This test might be less useful in busy clinical settings due to the demand for some math.
5. Clock Drawing Test (CDT) [44] and Mini-Cog [45]: The Clock Drawing Test (CDT) is used to diagnose frontal/executive, constructional praxis, and visuospatial dysfunction. The patient is instructed to draw a circle, after which the numerals are added to look like an analog clock face. The simplest scoring method was a three-point scale with one score for each of the following: a correctly drawn circle, numbers that are spaced correctly, and hands that display the correct time. At least 15 other scoring systems have been evaluated, some of which award over 30 marks. It usually just takes a minute or two to complete.

The Mini-Cog enhances memory testing by supplementing the CDT with a three-word recall test. It takes about 3 minutes to complete. When subjects draw a clock and cannot recollect any of the three words or can only recall one or two words and create an improper clock, they are categorized as having cognitive impairment.

6. The General Practitioner Assessment of Cognition (GPCOG) [46]: The GPCOG is comparable to the Mini-Cog in that it combines the CDT with a recall task (a name and location). Additionally, there are brief tests of orientation and recent event recall. In addition, a brief informant questionnaire is given to patients who received intermediate results on the first section. It should just take 5 to 6 minutes to complete. However, depending on how many patients complete the informant component, this estimate will change.
7. Clinical Dementia Rating (CDR) [47]: In one way, the Clinical Dementia Rating (CDR) Dementia is a three-point scale that is used to describe cognitive and functional performance in patients including Alzheimer's and other associated dementias. The CDR is based on a scale from 0 to 3: 0 indicates no dementia, 0.5 indicates emerging signs of dementia, 1 indicates mild cognitive impairment (MCI), 2 indicates moderate cognitive impairment, and 3 indicates severe cognitive impairment.

2.3.1 Gait Analysis and Cognition Decline

Dementia frequently goes hand in hand with diminished mobility. Some locomotor abnormalities may even take place before neuropsychological testing can identify cognitive deterioration. The examination of a person's gait may help to diagnose cognitive impairment. Memory loss and functional impairment are two important characteristics of

cognitive decline. Authors in [21] demonstrated that as cognitive loss advances, gait becomes slower and more variable using quantitative gait analysis with dual task paradigms. Particularly, gait cycle time variability rises in those with Mild cognitive impairment (MCI) and moderate Alzheimer's disease (AD) when cognitive dual tasking is contrasted with regular walking. Early identification of these mobility problems may be utilized as a diagnostic technique for people who are experiencing mild cognitive impairment.

2.4 Clinical Methods of Gait Analysis

A patient's gait is typically evaluated by specialists by making him/her walk and observing the quality of the patient's gait however, traditional scales are semi-subjective. They can be semi-subjective because following the walk sequence, the patient is often asked to rate the quality of his/her gait subjectively. Due to their subjective nature, these methods are disadvantageous for diagnosis, follow-up, and treatment of diseases, particularly with respect to accuracy and precision.

These traditional clinical methods usually consist of analyses performed by a specialist while the patients perform a few test walks in clinical conditions. The patient's various gait-related parameters are observed and evaluated while he/she walks on a pre-determined circuit. The following comprise a selection of the most common semi-subjective analysis techniques which are based on a medical specialist's observation of the patient's gait:

1. Timed 25-Foot walk (T25-FW): This is the first of three sections that make up the Multiple Sclerosis Functional Composite (MSFC), a standardized quantitative evaluation tool used in clinical investigations, particularly multiple sclerosis

clinical examinations [48]. During this exam, the expert counts how long it takes the participant to walk 7.5 m in a straight line which gives this test its name.

2. Multiple Sclerosis Walking Scale (MSWS-12): This scale evaluates 12 factors based on data from expert comments, literature reviews, and interviews with 30 patients that characterize the effects of multiple sclerosis on patients' gaits [49]. However, this exam was then modified to produce a general profile known as Walk-12 since various neurological diseases impair motor skills [50].
3. Tinetti Performance-Oriented Mobility Assessment (POMA): In this exam, the subject must move forward at least 3m, turn 180 degrees, and then rapidly return to the chair. Patients must use their regular walking aid if any, such as a cane or walker [51]. In a more recent study, Tinetti provided a simplified scale made up of seven factors with normal and abnormal as the two levels, which he claims properly reflects the risk of falls. The study of the human gait is based on nine additional factors that are divided into four levels in the full version of the exam, while the part on balance disorders is based on 13 parameters arranged in three levels. In conclusion, this test enables accurate assessment of balance and gait issues in senior people in real-world settings. The test does, however, take a lot of time and needs the subjects to actively participate.
4. Timed Get up and Go (TUG): Patients must stand up from their chairs during the timed TUG test, move a short distance, turn around, and return to their chairs before sitting down once more. [52]. The test is a robust and reliable method for measuring functional mobility that may also be helpful in tracking changes in clinical conditions over time.

5. Gait Abnormality Rating Scale (GARS): This examination of 16 aspects of human gait is based on video assessment. The GARS has seven categories for the trunk, head, and upper limbs, four categories for the lower limbs, and five general categories [53]. GARS is a quick and straightforward technique that assesses the link between gait anomalies and falls in the older population and predicts future falls.
6. Extra-Laboratory Gait Assessment Method (ELGAM): ELGAM is a technique for assessing gait in the community or at home [54]. Step length, pace, initial gait pattern, capacity to swivel the head while walking, and static balance are among the variables examined. Short steps, difficulty rotating the head, low speed (less than 0.5 m/s), and poor balance are all strongly associated with an unstable gait.

2.5 Automated Sensors based Gait Assessment

Contrary to the clinical methods explained in the previous section, the emerging technology trend in current world along with people's trust and reliance on technology, have given rise to several sensor-based algorithms which assist in an objective analysis of various gait parameters, leading to additional efficiency in measurement and providing specialists with enormous quantity of data on patients' gaits. This not only reduces the error margin caused by subjective techniques but also allows daily gait monitoring with no added efforts. These technology-based gait assessment methods can be broadly classified into two major categories: (a) Wearable sensors or obtrusive gait assessment as they are required to be worn by the person at all times, hence interfering with their daily lives; (b) non-Wearable sensors or unobtrusive gait assessment which are required to be installed and checked upon at regular intervals but do not interfere with daily lives.

2.5.1 Obtrusive Gait Assessment

This section of the thesis discusses some of the existing wearable sensor-based technologies of gait assessment whereas the next section elaborates on the existing technologies of non-wearable sensors and their limitations. As the name suggests, Wearable sensors systems requires the sensors to be placed on different parts of the body including feet, knees, thighs, or waist, usually in form of belts. Various kinds of sensors are used in these technologies to capture the changes in the signal as the subject walks, and these captured signals are then used to assess various gait parameters. Algorithms based on some of the most commonly used sensors under this category are discussed in following paragraphs.

Under the wearable category, inertial sensors are most commonly used. Inertial sensors are electronic devices that measure and report on an object's velocity, acceleration, orientation, and gravitational forces, using a combination of accelerometers and gyroscopes and sometimes magnetometers. As described in the reviews by Mobbs et al. [55] and Jarchi et al. [56], inertial sensors can be used to estimate walking speed by using a variety of methods. Studies such as Salarian et al.'s [57] aim to reduce the number of sensors on the body as a means of improving usability of these systems. In ambulatory gait analysis, they were also able to estimate thighs' movements from shank movements, reducing the number of sensing units needed from four to two.

Various muscles of a lower extremity can be studied using electromyography (EMG) by using surface electrodes or by inserting wires into the targeted muscle [58]. By analyzing EMG signals, it is possible to gain insight into muscle activity during gait. During movement, EMG analysis can be used to gauge the relative contribution of superficial

muscles. A gait analysis uses muscle activity information, such as timing the activities of the muscles and the strength of the muscles, to evaluate the walking performance of people with gait impairments. Using EMG at a prosthetic leg to predict initial movement, Wentink et al. [59] determined that the prosthetic leg can predict initial movement up to 138 milliseconds in advance in comparison to inertial sensors.

It is also possible to measure physical variables with sensing fabrics. Sensing fabrics are basically electronic components attached to the fabric's surface to measure physical variables. Research has shown that fabric-based wearables can detect gait abnormalities during daily walking for reconstructing postures based on previously-researched data [60], [61]. A plantar pressure distribution measurement and analysis system based on fabric sensors in shoes was described in Shu et al.'s paper [62] for gait analysis and balance control. We found that wearable devices based on fabric performed well in both static and dynamic measurements. An analysis system is provided by Changming Yang et al. [63] that used fabric sensors in pants and socks to monitor how people walk forward and backward or climb stairs.

2.5.2 Unobtrusive Gait Assessment

Non-wearable sensor systems also come with several options, which operate on varying principles. Using those as a basis, they have broadly classified them into three major categories: sound based sensor systems, light based sensor systems and force sensor systems. The most commonly used sensors under each category and recent related work for those sensors is elaborated in the following sections.

2.5.2.1 Sound Based Sensors

Sound based sensor systems are basically sensors which use sound waves for their operation varying from WiFi signals to ultrasonic waves and Doppler radar. Numerous research has been conducted using these signals to quantify mobility and patient monitoring in one form or the other.

Jia et al. in [64] proposed a target patch tracking approach on ultrasound videos to track the movements of bony structure as the test subject walks on a treadmill at the speed of 0.9 m/sec. The motive of research was to assist pathology research on musculoskeletal conditions, but same technology can be extended to perform gait assessment as well. Swati et al. in [65] also aimed to perform human motion analysis using ultrasound imaging by tracking the movements of femur bone. In this paper they propose a unique methodology to track bone edges and underlying bone displacement, which further indicates how different movement types affect internal bone movements. Extending the mobility assessment definition, authors of [66], proposed an ultrasound based technique to distinguish between an assisted and non-assisted exit from the bed which could severely affect the parameters like sit-to-stand timings and symmetry.

Besides ultrasound, other sound based methodologies are also proposed over time for gait assessment. Alshamaa et al. [67] proposed a Doppler radar-based method for the same where they emphasize on the importance of acceleration and deceleration zones of any walk. Authors in this paper studied walks conducted by 10 healthy young adults over a distance of 4.57 m at three different paces, and the gait speed was evaluated based on interclass correlation coefficient.

Authors of [68], [69] proposed an WiFi based daily activity monitoring system where they utilize the Channel State Information (CSI) of the WiFi signals to differentiate between the patterns of various dynamic human activities. Huan et al. in [70] also used CSI of the WiFi signals and achieved 95% of accuracy in gaits recognition. They used CP decomposition followed by Dynamic Time Wrapping to perform multi-variation activity recognition.

2.5.2.2 Light Based Sensors

Light based sensor systems, as the name suggests are sensors which rely on light for their operation. There is a huge range of such sensors like RGB cameras, RGBD camera, passive IR motion sensors, IR break beam sensors, TOF sensors, thermal cameras etc.

Time of Flight (ToF) sensor systems are based on cameras using signal modulation that measure distances based on the phase-shift principle [71]. Derawi et al. used ToF systems for human gait recognition by extracting gait features from the different joints and segments of the body [72]. In a recent study, Samson et al. used a ToF camera to analyse dynamic footprint pressures with high resolution [73].

Thermal camera technology is based on infrared waves and is known as Infrared Thermography (ITG). ITG is the process of creating visual images based on surface temperatures. It has the ability to accurately measure the infrared thermal intensity of the human body and its surroundings. This method was applied in [74] to recognize human gait patterns and achieved 78%–91% for probability of correct recognition.

The most obvious and common light based sensor is regular RGB camera. RGBD cameras provides additional dept information to the regular videos making them one of the popular choices among researchers. Several studies have been conducted using these cameras to monitor gait and calculate parameters like gait speed, stride length etc. despite the privacy

concerns raised by cameras. Mario et al. in [75] proposed a RGB video based analysis to assess various gait parameters including heel strike, toe-off, stride length etc. in turn differentiating between normal and abnormal walks. Authors in [76], [77] proposed a marker-less image processing algorithm for gait estimation. While the former used two RGB cameras to build a 3D model of the person walking using OpenPose library, the later used a single RGB camera and with the help of OpenPose library they tracked 2D coordinated of human joints. OpenPose is an open-source library used to identify anatomical landmarks using a CNN trained over data of images taken from a commercial camera. There have been several studies conducted [78], [79] to perform gait analysis using affordable depth cameras like Microsoft Kinect which allows to capture RGB and depth image simultaneously. Zhu et al. in [80] proposed a cellphone camera based approach to estimate stride length in turn monitoring patients suffering from Parkinson's disease with the help of a PVC mat which has markers printed on it. Though the method is scalable, portable and affordable, it can not be used for regular remote patient monitoring.

Passive infrared motion sensors are one of the most commonly used sensors in today's smart world and is a must in any smart home. These sensors provide accurate motion detection and have low battery usage which makes them perfect for regular remote gait assessment. Motion sensors have been used to detect activity [81], [82] during nighttime in patients of dementia to alarm their caregivers in case of any unwanted incident. Numerous multi-sensor home monitoring systems are currently being tested, including those that measure gait speed. Currently, the CART [83]–[85] sensor system uses a series of motion sensors positioned in a straight line on the ceiling with fixed spacing between them. In the CART initiative, researchers seek to facilitate the independence and health of

older adults within their diverse communities over a long period of time. CART uses innovative technology to enhance research into aging in place.

2.5.2.3 Force Sensors

The Force sensors are called as such due to their nature of collecting information based on amount of pressure and Ground Reaction Force (GRF) exerted on them. There is numerous research conducted using these types of sensors where they are laid down on the floor and test subjects are asked to walk on top of them. These generally include pressure sensors embedded in the form of pressure sensitive mats or force plates.

Samadi et al in [86] developed an innovative method to accurately assess the vertical various components of GRF under each foot using a large force platform placed on the ground which can help with various health monitoring such as abnormal posture, fall prevention etc. Authors in [87] managed to achieve the same feat of total GRF evaluation using three basic force platforms, cutting the cost by a huge margin and thence improving the feasibility of the method.

Fadi et al in [88] used a 4.9m long electronic pressure mat where they observed the active pressure sensors as any individual walks over them. The location of these active sensors was then used to assess the gait parameters like walking speed, stride length, stride timing etc. Mobility assessment using pressure mats is not limited to gait parameters but mobility of bedridden patients can also be monitored by placing a pressure sensitive mat under the mattress as achieved by the authors of [89]–[91]. Authors in these papers not only manages to quantify the mobility in bed ridden patients, but also parameters like sit-to-stand timing of patients and center pressure point while they stand, such parameters are specifically helpful in monitoring a patient under rehabilitation.

2.6 Summary

Gait analysis is extremely useful for determining the severity of gait disorders, distinguishing between peripheral and central nervous system disorders, and identifying motor abnormalities, particularly in dual-task situations like home settings in elderly people with gait disorders or memory impairment. It was concluded that older persons with early cognitive impairment are also more likely to have worse gait smoothness in addition to the recognized alterations in gait speed and step length. The time and money needed to conduct a study and interpret it are the biggest obstacles to clinical gait analysis [92]. In contrast to other clinical tests, "gait" reports are extensive, contain poorly understood data, and requires a clinical interpretation which could be subjective in nature. In order to solve these issues, current research is developing methods for quickly, precisely, and efficiently capturing data and for interpreting it using a variety of modelling, statistical, wave interpretation, and artificial intelligence technologies. Our technological prowess and the interaction between engineers and clinicians are both crucial for the success of such initiatives. As a result, a large number of studies and research projects have been carried out in the field of ambient gait monitoring using the wearable and non-wearable sensors as listed in this chapter. Even if they are capable, wearable sensors have a number of drawbacks, the main of which is the design and technology difficulties that drive up the cost of these devices. The major issue that still exists for the continuous monitoring of present or potential cognitive patients is their forgetfulness to wear the sensor itself. On the other hand, non-wearable sensors offer a way to solve this problem and have good potential in doing so. However, the majority of these technologies are currently heavily reliant on the lab environment. As a result, they

are not ideal for routine, day-to-day gait monitoring. In addition, they are unobtrusive in the sense that they are not required to be worn by the patients but are not really ambient in a home setting which might discourage some people against installing them in their homes. This creates a place for innovative technologies or solutions that can address both problems at once. Following chapters of this thesis are devoted to experiment with such technologies.

Chapter 3: Evaluating changes in Gait and Activity Associated with Cognitive Impairment

3.1 Introduction

Changes in mobility are closely associated with health decline in older adults including their cognitive abilities. Extending the same idea, mobility is frequently assessed in the clinic setting at episodic intervals during recommended regular health checkups of older adults. As the motivation behind this thesis goes, passive sensors within a smart home setting allows for unobtrusive collection of daily activity data which can be further used to analyze mobility and gait information over an extended time period. This method of high frequency data collection in comparison to the traditional clinical ways could be sensitive to early changes in mobility associated with cognitive decline which can help with early detection and help reduce further decline with appropriate medical assistance. One of the significant parameters for health and well-being monitoring is gait, big data analysis presented in this chapter is trying to use these passive smart home sensors and link the data collected from them to the cognitive decline in older generations. The following section explains to experimental setup used during this test.

3.1 Gait Line

Passive Infrared Motion sensors have been well researched to accurately detect human motion within a specific area range and are currently installed in several houses serving various practical applications. These sensors are generally connected to hub via Personal Area Network (PAN) which is a type of wireless communication network and the most

used protocol among these sensors is Zigbee protocol. Zigbee is a very popular choice among the sensors networks and plays a prominent role in the current IoT market. Its low-cost and low-power nature alongside with better security options are the major reasons behind its popularity, which adds additional points towards the feasibility of the motion sensors. Keeping these features in mind, the Collaborative Aging Research using Technology (CART) system designed a setup containing 4 motion sensors attached to a ceiling in a sequence, equally spaced from each other with the idea that further processing of these sensors' data would allow to extract the time taken to walk a fixed distance.

3.1.1 Sensor Deployment

The CART Initiative platform includes a variety of motion and contact sensors that are deployed in the homes of participants. As shown in Fig. 3.1, there are four of these motion sensors installed in a continuous corridor measuring 1.83 m (6 ft) in length and each being 0.61 m (2 ft) apart from each other. These sensors' intended use is to measure gait speed by measuring the intervals between each sensor's triggers. The gait sensors in use are the NYCE Curtain Motion Sensor (NYCE Sensors, Burnaby, BC), which has a 5 m detection range and can detect any motion that is occurring inside a 20°/90° cone. They are often fixed on the ceiling and positioned so that the 20° direction aligns with the vertical length of the hallway and the 90° direction spans the width of the corridor. According to Fig. 3.1, a resident walking down the hallway should activate the sensors in the following sequences: 1, 2, 3, 4, or 4, 3, 2, 1, depending on the direction of the walk.

The gait line and other sensors are connected to the Raspberry Pi PC, which serves as the network's hub, where communication is performed through the Zigbee wireless protocol.

The PC receives the sensor-generated events and timestamps them. After that, the PC sends the information to the secure data centre for any additional analysis.

The motion sensors used are PIR motion sensors in nature which consists of 2 slots for special IR sensitive material. Both slots detect same amount of IR in idle environment however there is differential change between the two halves if there is a motion in is proximity. These asynchronously sampled motion sensors send a motion event to the hub when they detect motion and a "no-motion" message to the hub if they don't detect any motion for five consecutive seconds. The sensors do not send repeated "motion" messages when they notice prolonged continuous motion.

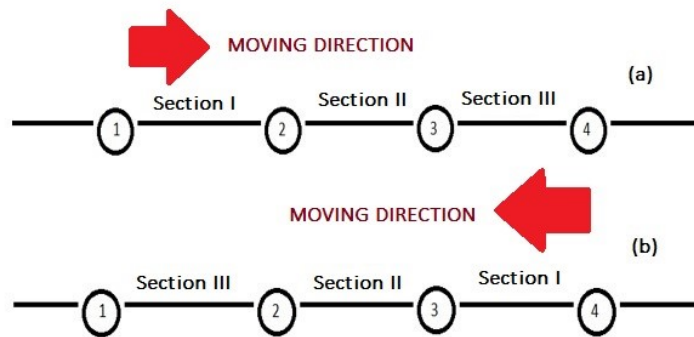


Figure 3.1 Illustration of Gait Line and section definition

3.1.2 Data Acquisition

More than 300 older adults residing in several locations of the United States and Canada are registered with the CART sensor platform and have it installed in their homes. These elderly people may or may not be living alone. Data from 32 households distributed in the USA was examined for the first trial. With a ubiquitous sensing and computer system installed in their homes, all 32 of these residences are occupied by a single person who is a participant in the CART Initiative for aging research. 16 of these 32 people score 0.5 on

the Clinical Dementia Rating (CDR) scale (MCI), while the remaining 16 score 0 on the CDR scale (HC). Eighty percent of the subjects observed in this study lived in low-income senior residences, and six percent were non-white. The 6% participating elders were non-white. The groups were matched by age, sex, and education. Each participant's initial 100 days of data from the day of their program enrolment, which was also the day the CDR scores were assessed, were considered for this study. This step was taken instead of matching the same dates for each participant, only to avoid any discrepancies as CDR scores may change over time.

3.2 Preliminary Data Analysis

3.2.1 Data Cleaning

The comprehensive set of data from all the sensors installed in any residence is saved in a database that is obtained from the hub and is used for this analysis. To make this data available in a MATLAB data structure that can be thoroughly analyzed, pre-processing was performed on the original .csv files. The pre-processing includes many steps, other than CSV to MATLAB data conversion it includes converting sensor IDs to readable sensor names for easy understanding, deciphering of coded messages sent by sensors, deletion of unnecessary information etc. This file included both "motion" and "non-motion" events, as suggested earlier. The "motion" events from the gait line-specific sensors were then the only ones left after filtering out the other sensor events. In this procedure, it was noticed that data sequences like those in Fig. 3.2 (a), where one sensor failed to communicate the message and Fig. 3.2 (b), where four sensor events are all present within a constrained time range but may or may not be in chronological order. There were

also instances where messages from other sensors were interposed between these sensor line messages, and such messages were taken out during the cleaning procedure.

28-Apr-2020	15:24:52.753	line4
28-Apr-2020	15:24:53.553	line3
28-Apr-2020	15:24:54.440	line2
28-Apr-2020	15:25:26.219	line4

(a)

28-Apr-2020	15:28:21.543	line4
28-Apr-2020	15:28:23.043	line3
28-Apr-2020	15:28:23.823	line1
28-Apr-2020	15:28:24.278	line2

(b)

Figure 3.2 Screenshot of pre-processed data (a) Missing sensor event (b) Out of order event

3.2.2 Observations on Cleaned Data

During the experiment many observations were made which indicated abnormal behaviour of the gait line sensors. It was noted that in many instances only two or three out of four gait line sensors reported any activity as seen I Fig. 3.2 (a), which is otherwise impossible as the sensors were placed in an uninterrupted hallway. According to general architecture of the houses involved, it was practically impossible to trigger any two sensors while not triggering others. It was also noted that not every time when a person walked beneath the walking line, the sensors were reported to be triggered in the expected sequence of 1,2,3,4 or 4,3,2,1. Due to area covered being a hallway, the only way possible to walk beneath these gait line sensors is to walk from one end of the hallway to another and hence comes the expected sequence. Out of order events as seen in Fig. 3.2 (b) pointed out towards an unusual and unexpected behaviour. Another intriguing observation was that often only some of the four sensors were reported to be triggered on the other hand sometimes sensors

were reported to be triggered while there was no activity reported by others. An extensive experiment was conducted to analyze the exact reason behind this which is explained in the following chapter. But all these observations indicated towards incorrect gait speed calculation, therefore in order to minimize thesis concern with the data, number of walks was estimated as a measure of mobility instead of a measurement of gait speed. However, the need to define the definition of walk still pertains based on sensor operation.

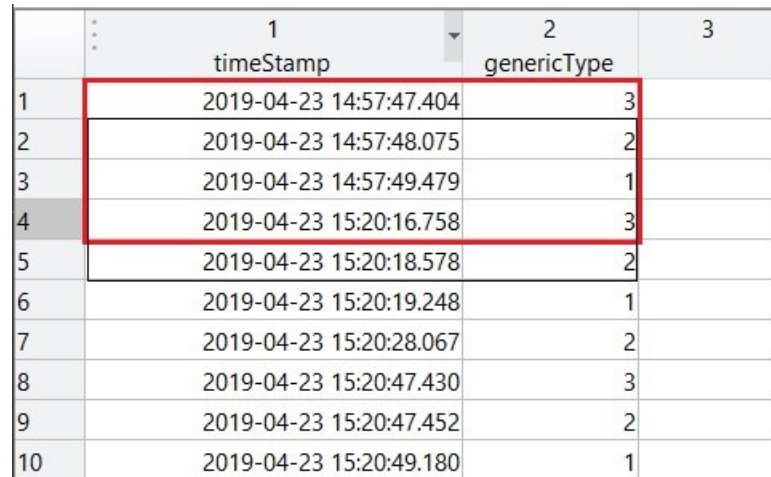
3.3 Identification of Walks

The first step towards walk redefinition is to let go of the importance of chronological order since event reordering was a common feature observed in the data. Based on the information collected so far, it was concluded that there were three major questions to be answered before deciding on an optimal definition of walk:

1. If reported 3 out of 4 sensor events are sufficient to conclude that a walk occurred or triggering of all 4 sensors is crucial?
2. What is the optimal time limit between all sensor event so that events with prolonged time are not excluded but two consecutive events are not merged?
3. Since sensors do not report 2 messages if it detects 2 walks within a very short time gap, is it possible for 1 reported sensor triggering event to be a part of 2 different walks?

The algorithm to check the “walks” was designed around a window of size 4 which iterates over the pre-processed and filtered data with a step size of 1, however if 1 sensor event should only belong to 1 “walk”, the step size would change if a walk detected to skip the events now associated with that walk. The data captured within the window is analyzed to

estimate how many of the line sensors were reported to be triggered, and time difference between first and last events was calculated to check if the events occurred within the time limit. The window and its movement are illustrated in Fig. 3.3.



	1 timeStamp	2 genericType	3
1	2019-04-23 14:57:47.404	3	
2	2019-04-23 14:57:48.075	2	
3	2019-04-23 14:57:49.479	1	
4	2019-04-23 15:20:16.758	3	
5	2019-04-23 15:20:18.578	2	
6	2019-04-23 15:20:19.248	1	
7	2019-04-23 15:20:28.067	2	
8	2019-04-23 15:20:47.430	3	
9	2019-04-23 15:20:47.452	2	
10	2019-04-23 15:20:49.180	1	

Figure 3.3 Screenshot illustration of window and its movement

Based on the three questions, following six different definitions of walk were created and compared within the research team:

Case 1:

Condition 1: All 4 sensor should be present regardless of the order

Condition 2: Sensor events must all occur within 10 sec

Implication: Two sets of sensor events that overlap (share some but not all sensor events) could be counted as two or more walks.

Case 2:

Condition 1: Any 3 out of 4 sensors should be present regardless of the order

Condition 2: Sensor events must all occur within 10 sec

Implication: Case 1 but with a relaxation that 1 of the 4 sensors can be missing

Case 3:

Condition 1: All 4 sensor should be present regardless of the order

Condition 2: Sensor events must all occur within 6 sec

Implication: Case 1 but with a tighter time limit

Case 4:

Condition 1: Any 3 out of 4 sensors should be present regardless of the order

Condition 2: Sensor events must all occur within 6 sec

Implication: Case 2 but with a tighter time limit

Case 5:

Condition 1: All 4 sensor should be present regardless of the order

Condition 2: Sensor events must all occur within 10 sec

Condition3: Adaptive step size,

Implication: Case 1 but with "adaptive step size" which means that when first 2 conditions are met and data within the window is confirmed to be a "walk", step size is changed to 4 i.e., any sensor triggering event can't be included in more than 1 "walk".

Case 6:

Condition 1: Any 3 out of 4 sensors should be present regardless of the order

Condition 2: Sensor events must all occur within 10 sec

Condition3: Adaptive step size,

Implication: Case 5 but with a relaxation that 1 of the 4 sensors can be missing

After the discussion, Case 6 was concluded to be the best option since missing sensor events was a common occurrence justifying the condition 1 of Case 6. Based on the typical walking speed of adults over 80 i.e. 95cm/sec [93] which adds up to ~2-3 sec for a 6ft walk and the delay caused by communication between the sensors and the hub, the time frame

of 10 seconds was chosen justifying our condition 2. This concept of communication delay can be understood based on the observations of the following chapter. Not too many cases where one sensor event belongs to 2 consecutive walks should occur as that would only happen if residents walked up and down the corridor instantly. On the other hand, allowing one sensor event to be included in multiple walks could lead to potential fake walks especially in this messy data. Hence, in order to simplify things and to not recognize fake walks due to events reordering, adaptive step size was chosen. Since the aim of this experiment was not to calculate the precise walking speed but rather to analyze the mobility and link it to the cognitive abilities, this compromise is acceptable. Fig. 3.4 shows walking activity of resident from one sample house for all the weeks under observation as calculated using the 6 definitions explained above. It can be observed from the plot that allowing a time margin of 10 sec and one sensor event to be included in multiple walks raises number of walk events significantly.

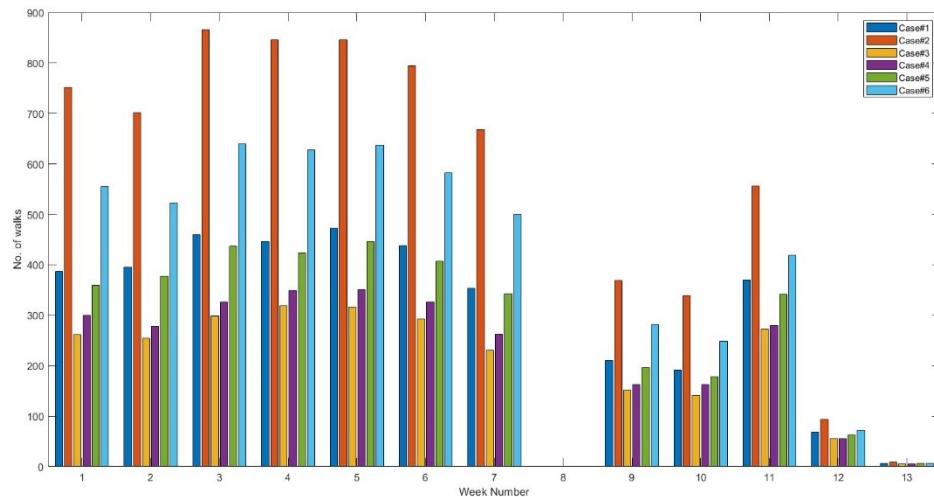


Figure 3.4 Number of walks per week according to all 6 definitions for a sample home

3.4 Results

In addition to the CDR scores, the MoCA scores of all participants were calculated as a measure to their cognitive abilities which is explained in detail in Chapter 2. Participants with a CDR score of 0 had a mean age of 72.1 years and a mean MoCA score of 26.1 with a range of 21 – 30. Participants with a CDR score of 0.5 had a mean age of 72.2 and a mean MoCA score of 22.1 with a range of 15 – 27. Fifty-six percent of participants in each group were female. Preliminary data from the gait line from a combined 1400 days for CDR0 participants and a combined 1250 days for CDR0.5 participants is presented in the following plots shown in Fig. 3.5 and 3.6 as for many participants, they were not home or technical issues causes days with no gait line data. It was observed that the mean number of daily walking events detected by the gait line was significantly greater for CDR 0 participants (101.4) compared to CDR 0.5 participants (92.8). This is also reflected in the following plots. The cyclical pattern for CDR 0 shows that daytime activity surges around early morning and dinner whereas nighttime activity is calmer, however for CDR 0.5, the pattern is flatter with greater nighttime activity and significantly fewer daytime activity spikes.

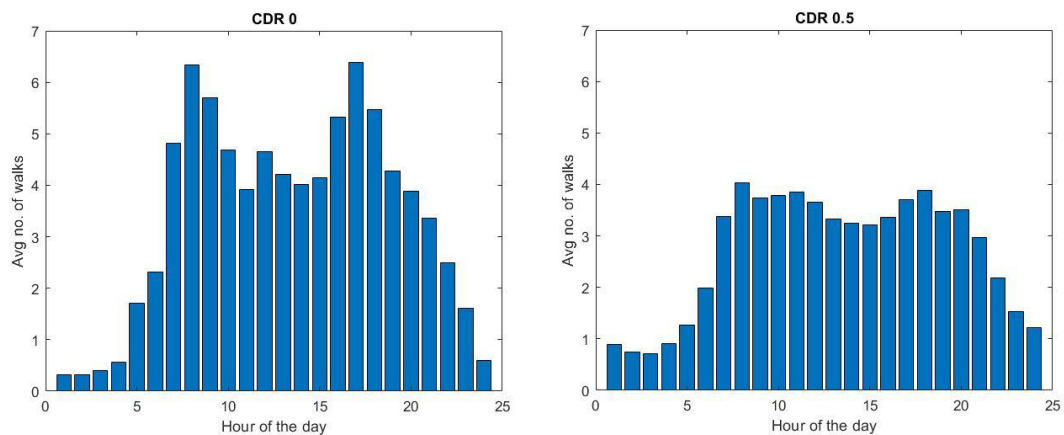


Figure 3.5 Average number of walks per hour over a day

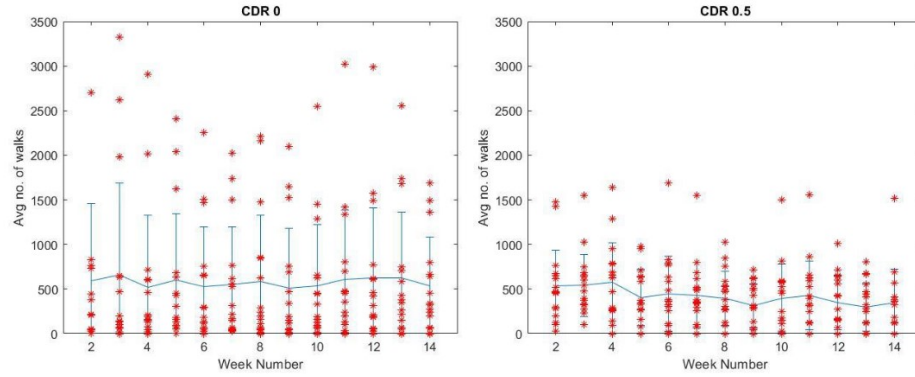


Figure 3.6 Average number of walks per week over a 3-month period

3.5 Conclusion

Based on the experiment conducted in this chapter, passive sensors are able to collect data on gait and activity levels in individuals with a technology platform deployed within their home on a regular basis. As noted from our observations, this unobtrusive remote mobility assessment methodology has the potential to identify individuals experiencing cognitive impairment which establishes our goal. Differences in activity level were observed in individuals with mild cognitive impairment compared to those with normal cognition. Medical studies [94], [95] that links MCI with disturbed sleeps, overnight awakenings, and in certain cases nocturia supports the differences in sleeping patterns as seen in patients with CDR group 0.5 and CDR group 0 individuals. Thence, when continuously observed over time, these sensors have the capability to detect any decline in mobility and hence the cognitive abilities.

However, at the same time the experiment highlighted some anomalies in the data reported by these passive sensors to their hub which could pose serious concerns when it comes to precise walk speed assessment. The experiment explained in the following chapter was designed to determine the root cause of these anomalies.

Chapter 4: Using Zigbee Sensors for Ambient Measurement of Human Gait – Analytical Considerations

It was noted in the previous chapter that not always do these sensors report their event in ideal manner and the data collected from the hub is far from what one would imagine it to be. This chapter starts by assuming that no such anomalies exist and then work our way up to detect them and analyze their origins.

4.1 Experimental Setup

The experimental setup used in this chapter is fundamentally same as the one explained in previous chapter. To simplify the experiment and analyze the depths of data anomalies in detail, instead of the original 32 homes as explained in section 3.1.2, the gait line data was explored for the 3 houses located in Ottawa, Canada that the local research team was directly responsible for including installation of the sensors. Each of these three houses had 2 residents: an older adult and a care giver.

After similar anomalies in the collected data from these homes was established, an additional experiment was performed in a research team residence amid the COVID lockdown and inaccessibility of lab space. In this experiment, along with the gait line created by NYCE motion sensors which is used in CART sensor systems, an identical gait line was created using Samsung SmartThings motion sensors.

The supplementary experiment was conducted to obtain comparable data but in a controlled manner because the sensor data for the trial households were acquired in an unpredictable and unobserved environment. This was accomplished utilising a gait line composed of four NYCE Curtain Motion sensors that were identical to those used in CART

homes. In addition, the Samsung SmartThings system, which also use the Zigbee protocol, was installed by placing each of its four motion sensors next to a NYCE sensor. Again, 0.61m between each pair of sensors was used in the deployment.

The test subject performed several slow test walks at comparable speeds with a straight posture, relatively slow walking pace, a short stride length, and no arm movements. Utilizing the latter two helped to reduce variations in the body's front surface such as early sensor tripping due to extended arm movements. The data from both systems was entered into databases, with the Samsung system implemented using a cloud storage method and the NYCE sensors using the same database system as employed in the CART households.

4.2 Ottawa Residences' Data Analysis

The analysis described in this section is based on a naïve approach which does not consider any noise factors such as early tripping of sensors, transmission delay or missing events, however, is sufficient to give a basic idea about their functionality. The data is stored in a database which is retrieved from the hub and includes the extensive set of data from all of the sensors including those other than the gait line. This data was pre-processed following the same steps as explained in section 3.2.1. The resulting data set was analyzed to find all gait line walks defined as a sequence of triggers of the 4 motion sensors (1,2,3,4 or 4,3,2,1). The definition of walk was considered as such since time difference calculations are pointless for jumbled events. Based on this definition, event captured by screenshots shown in Fig. 4.1 (a) and Fig. 4.1 (b) are classified as non-walks however that of Fig. 4.1 (c) is considered a walk. The time taken to walk 1.83 m was calculated from these resulting gait line events by analyzing the total duration between the first and last sensor tripping event. A sub measure of the time to walk each of the 0.61 m segments, the time between each

sensor was also measured. The internal segment variation was examined, and any walks with a variance more than 2 sec^2 which would essentially indicate a mid-walk stop were disregarded. To see if there were any trends in the data, scatter plots and histograms were produced which are discussed in the following section.

2019-08-22 14:06:33.509	'Line2'	'motion'	1
2019-08-22 14:06:34.002	'Line1'	'motion'	1
2019-08-22 14:06:34.476	'Line3'	'motion'	1
2019-08-22 14:06:34.701	'Kitchen'	'motion'	1
2019-08-22 14:06:35.176	'Line4'	'motion'	1
(a)			
2019-08-22 14:07:30.707	'Line2'	'motion'	1
2019-08-22 14:07:31.290	'Line1'	'motion'	1
2019-08-22 14:07:31.967	'Line3'	'motion'	1
2019-08-22 14:07:32.993	'Line4'	'motion'	1
(b)			
2019-08-22 14:07:59.954	'Line4'	'motion'	1
2019-08-22 14:08:02.984	'Line3'	'motion'	1
2019-08-22 14:08:03.830	'Line2'	'motion'	1
2019-08-22 14:08:05.350	'Line1'	'motion'	1
(c)			

Figure 4.1 Screenshot of pre-processed data (a), (b) Classified as non-walks (c) Classified as walk © 2021 IEEE

4.2.1 Observation and Discussion

Figure 4.2 displays the findings for one of the sample homes where the results are displayed as a histogram of the internal gait line segment time intervals and the total gait line time for walks in a single direction, where classes for individual segments are determined over periods of 0.1 s and 0.2 s, respectively. Where, first segment during any walk would be the section between first 2 sensors which the resident walks by irrespective of the direction of walk, this is explained using an illustration in Figure 3.1. The same analysis and presentation are shown for walks going in the opposite direction in Figure 4.2(b). Figure 4.2 (a) shows the findings for more than 1000 walks, whereas Figure 4.2 (b) shows the

results for over 5000 walks. A first indication of a potential data discrepancy is the imbalance of the number of walks in the two opposite positions.

Analysis of the histograms for the total time taken to walk the hallway in Figure 4.2 (a) and Figure 4.2 (b) (bottom graph in each) reveals that both cases approximate a normal distribution, which could be the desired outcome. However, the two distributions are concentrated around different mean values, which is unexpected given that the participants were the same and walked in the same hallway but simply in two different directions, therefore the time taken to walk the distance should be similar.

In Figure 4.2 (a), where the subsections have significantly varied distributions, a closer look at the histograms for the interior segments reveals some extremely perplexing results. It reveals that residents typically take 0.6–0.7 seconds to cross section 1 (the distance between line sensor 1 and 2); therefore, it would be reasonable to assume that they would spend a comparable amount of time to cross the other 2 segments of the walk line. In other words, if the time difference for section 1 is between 0.6 and 0.7 s in the majority of the walks, then the time difference for all of those walks should be between 0.5 and 0.8, i.e., the peaks for bin 0.5-0.8 should be the largest. All four histograms of Figure 4.2 (a), however, present a different picture, pointing towards a problem with the recorded data. It is doubtful that anyone, much less an elderly person, would walk naturally while accelerating/decelerating to this amount over a distance of just 0.61 m.

Figure 4.2 (b) did not immediately highlight the issues shown in Figure 4.2 (a), although the segment 1 histogram differs significantly from segments 2 and 3. The only difference in these results from the same house and people was the walk direction, which was observed for the same number of days. This divergent behaviour displayed by the two

graphs is just another sign of a measurement problem. The data from Figure 4.2 (b) is presented in Figure 4.3 as a scatter plot, where the three coordinates are represented by the time difference between the three sub-sections. Given that the time for each of the three segments is anticipated to be correlated, they should ideally form a straight line ($x = y = z$). For reference, a blue line denoting the line is displayed. Instead, the ensuing scatter plot for the segment timings exhibits virtually no association, which in itself is another sign of an underlying measurement problem.

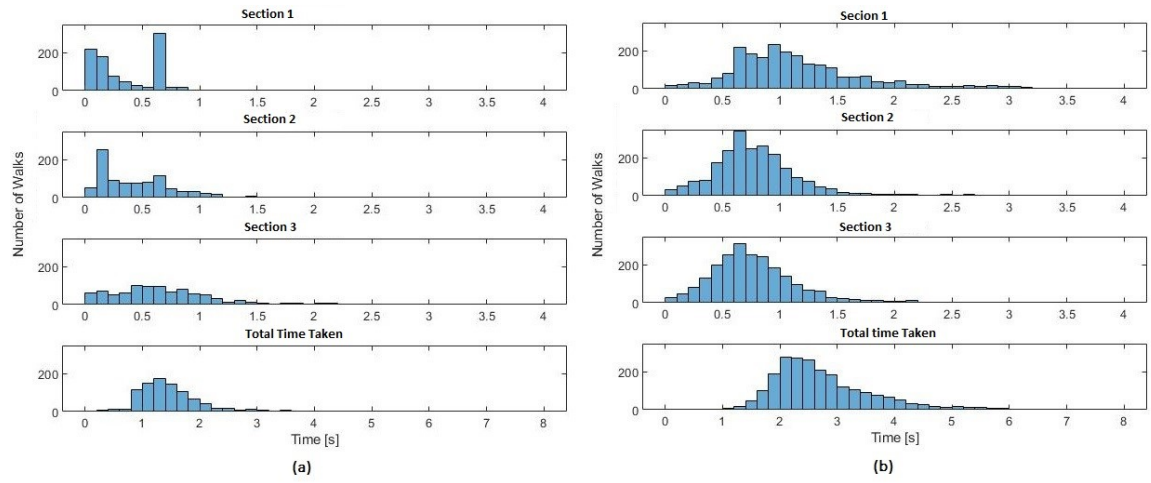


Figure 4.2 Histogram of time intervals for House 1 in direction (a)1 to 4 (b) 4 to 1 © 2021 IEEE

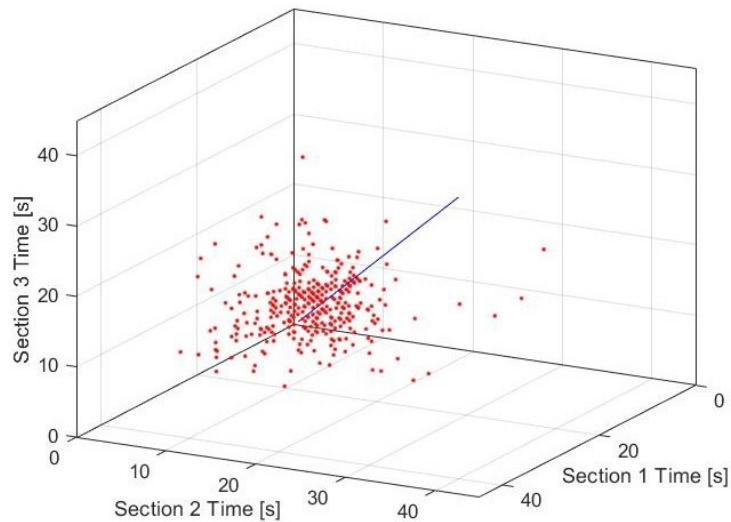


Figure 4.3 Scatter plot of time intervals in direction 4 to 1 for House 1 © 2021 IEEE

As a result, several of the observations in Figure 4.2 were needed to be reconsidered. It became crucial to consider the possibility that the out of order events might actually be a more severe representation of underlying problems with the internal interval timings as they were observed frequently and similarly across all houses under observation. These anomalies could have been caused by varying reasons such as house topography, sensor not working properly, etc. but it is unlikely for these issues to be consistent across all houses. The layout of the house in conversation is shown in Figure 4.4, which makes it clear that house topography is not an issue in this particular case such as the sensor line have a hallway end or door at one end.

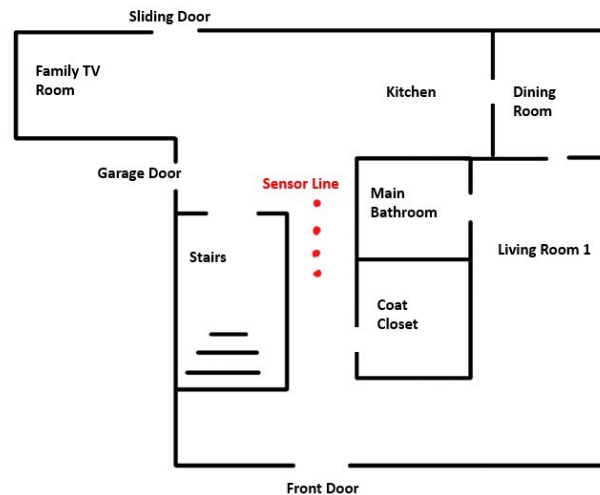


Figure 4.4 House layout map for the sample house in conversation

There could also be delay in detection of the event itself by the sensor if the second walk occurs within 5 secs of previous walk, but anomalies were noticed otherwise as well. This gave rise to the hypothesis that there might be difficulties with the sensors accessing the Zigbee wireless link that are related to the fundamental workings of the communication protocol. The presence of additional sensors with the gait line sensors sequence suggested that results may have been impacted by competition in the wireless communication traffic.

Referring to Figure 4.1(c), for instance, even if the motion sensor event from the living room was filtered out, it was still transmitted via the Zigbee network between the messages for line sensors 2 and 3, potentially increasing the lag between the two gait line sensors. Concerns are also raised by Figure 4.1 on the reason why there are so many instances where all 4 sensor events are present in a brief period of time but are not recorded in the normal order.

4.3 Controlled Experiment Data Analysis

This controlled experiment was carried out in order to dispel various doubts, such as whether these discrepancies were brought about by the uncontrolled nature of the data collection process and whether the outcomes might differ if the same experiment were carried out in a lab setup without the presence of any other additional sensors. The walk line installed in research team member's home had added distance towards both the ends of the walk line, so sudden starts or stops were not made during the walk or near to the walk line and they were timed to be at least 5 secs apart. In this experiment, the same algorithm was employed as in the test homes, to assess many controlled walks that were recorded by both sets of sensors. The outcomes for these walks are compiled in Table 4.1, which shows the total time recorded by both sets of sensors for six different walks when the 4 sensors were captured in the anticipated order. Even in this well controlled scenario, there were out of order sensor events that aren't listed in his table resulting in the six walks described, in turn indicating the existence of additional noise or fluctuations. The difference in total time provided by the two sensor systems is displayed in the table's fourth column. For a distance of 1.83 m, a time inaccuracy of 100–800 msec can result in a walking speed error up to an estimate of 2.3–18.3 m/sec. Hence it can be concluded from

the results of this experiment that reordering of events and internal delays in the communication of the sensors to their hubs is still present even if there are no additional sensors paired to the hub. After eliminating any other possibilities, the Zigbee protocol was examined to determine how it might be influencing the precision of the time stamps and sensor communications as a result of the large variation in the observed value.

Table 4.1 Total time recorded by both set of sensors and their difference © 2021 IEEE

Walk Number	Duration Recorded (sec)		Difference
	<i>NYCE</i>	<i>Samsung SmartThings</i>	
1	3.445	2.729	0.716
2	3.237	3.345	-0.108
3	2.834	2.532	0.302
4	2.779	2.631	0.148
5	2.55	3.394	-0.844
6	3.811	3.358	0.453

4.4 Zigbee Protocol Analysis

It is necessary to first comprehend why the bulk of ambient sensors on the market today use the Zigbee communication protocol in order to fully grasp why Zigbee communication concerns are so crucial for not only our data analysis but in general. IoT networks must take into account the special needs of cheap, low-power wireless networking. A wireless technology called Zigbee was created as an international standard to accomplish these needs. The Zigbee standard uses IEEE 802.15.4 [96] as the physical radio specification and works in unlicensed bands like 2.4 GHz and 900 MHz. The 802.15.4 specification, which serves as the foundation for Zigbee technology, was approved by the IEEE (Institute of Electrical and Electronics Engineers) in 2003. Zigbee is a packet-based radio protocol that

was developed for low-cost, battery-powered devices. Devices that support Zigbee have lengthy battery lives that can sometimes last for years while also being able to communicate in a variety of network topologies. Zigbee has a variety of benefits, some of which are listed below:

- Zigbee has a flexible network topology that enables it to connect to more devices with a lower chance of harm to other connected devices in cases of malfunctioning of one connected device.
- It also has a very long battery life because Zigbee transmission uses very little power and goes to sleep mode when not in use, giving users the convenience of not having to change the batteries frequently.
- The most well-known wireless communication technology, Zigbee has a mesh network topology and offers low-cost, multiple-hop data transmission.
- Zigbee supports a large number of nodes, allowing it to be connected to more devices, making it ideal to be used in a smart home setting where multiple sensors are installed to complete even the smallest of the tasks.
- The Zigbee algorithm is much less complex than Bluetooth, making it easier to understand and implement.
- It is simple to install, making it easier for people with non-technical background to make use of in practical life scenarios.

4.4.1 Intro to Zigbee Protocol

A Zigbee network is made up of several sensors, at least one Zigbee hub/router, and is known as a personal area network (PAN). Any specific PAN can be configured to operate

in either Beacon mode, where it sends out periodic beacons for all communications, or non-Beacon mode, where the hub maintains its receivers active at all times. A Zigbee hub/router that is set up in beacon mode uses a superframe structure to connect with any additional routers and end-point sensors. An example of the superframe structure is shown in Figure 4.5. This superframe structure starts with a beacon frame and is followed by an active and inactive period. For the purposes of this analysis, it is assumed that the inactive period is 0 respecting the default values as the inactive duration for sensors in use is unknown. If this value is not zero, less time will be available for communications, which will further impair system performance. Superframe Duration (SD) refers to the total amount of time needed for beacon transmission and the active phase, whereas Beacon Interval (BI) includes both the SD and the inactive intervals. The term "BI" will be used in the following discussion since, under the zero-length inactive period assumption, SD is equivalent to BI in our situation.

The standard divides the super frame's active area by default into 16 equal slots known as contention access periods (CAP), which may or may not be followed by a contention free period (CFP).

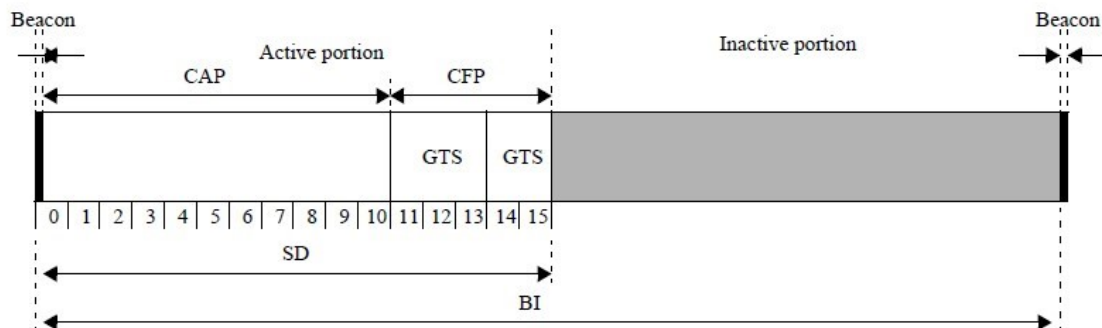


Figure 4.5 Example of superframe structure sourced from IEEE Std. 802.15-4 Figure 6-1 © 2020 IEEE

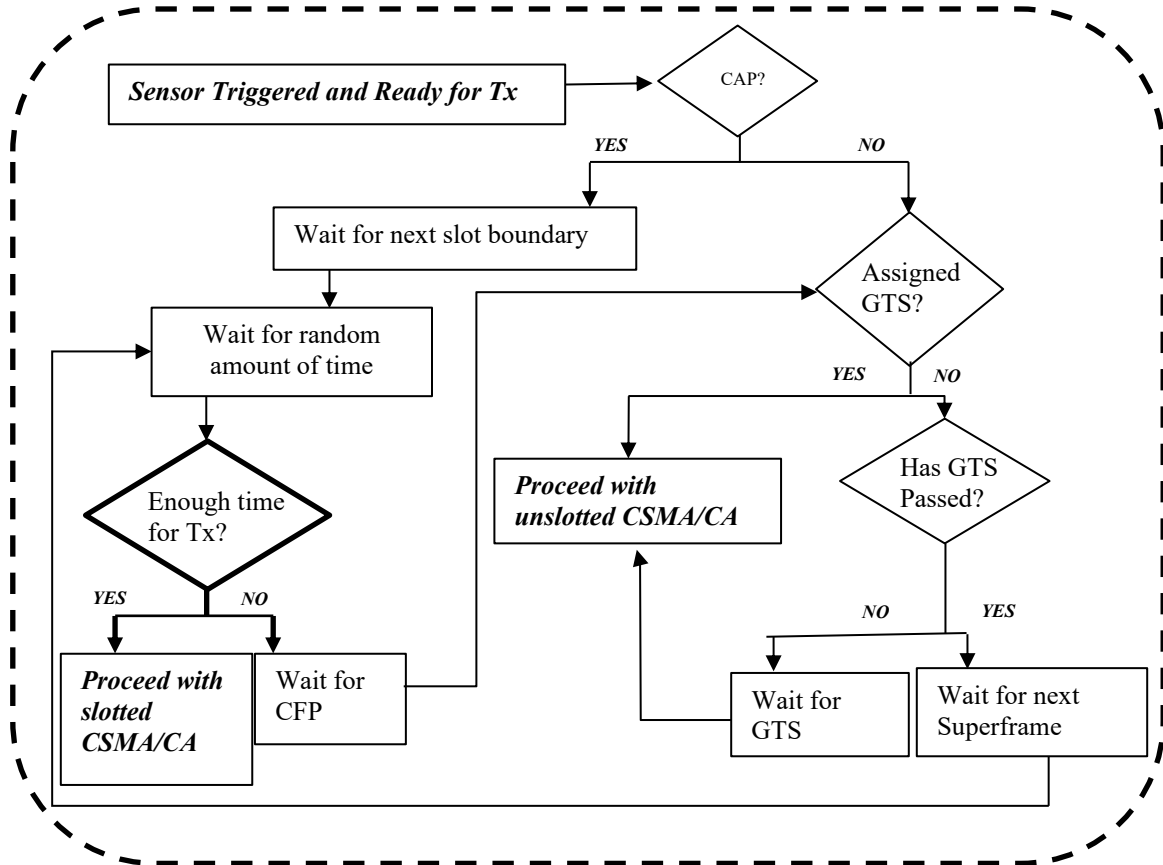


Figure 4.6 Flow Chart depicting process any sensor undergoes while transmitting a message to the hub

All network-connected devices use the same channel to send and receive data, which can cause conflict if two devices try to send data at the same time. By giving specific network sensors Guaranteed Time Slots (GTS), each of which includes one or more slots, CFP limits the likelihood of contention. Assigned sensors must complete transmitting and receiving the acknowledgement frame within one Intraframe Spacing (IFS) during one GTS. The configuration of the PAN determines the number of GTS assigned and, consequently, the length of CFP, which may be zero, meaning that no GTS are assigned to any sensors.

Any sensor in CAP is free to communicate data at any time, but this procedure may still experience congestion if two or more sensors attempt to send data at the same time and a collision takes place. When configured in Beacon mode, all data transfers in CAP employ the slotted Carrier-sense multiple access with collision avoidance (CSMA/CA) technique, however unslotted CSMA/CA is used when in non-Beacon mode.

Unslotted (Beacon mode) and slotted (non-Beacon mode) CSMA/CA implementations of the standard differ significantly in the sense that slotted CSMA performs Clear Channel Assessment (CCA) twice during each transmission attempt, but unslotted CSMA performs CCA only once. The Chapter 6 of IEEE Standard 802.15-4 provides a thorough discussion of both slotted and unslotted CSMA/CA algorithms.

The process followed by any end point sensor trying to communicate with the hub after being triggered is shown in the flow chart in Figure 4.6, which describes the transmission model in the standard and assumes CFP length to be zero. The process is carried out in an effort to minimise power consumption and handle any potential collisions. The degree of delay added by this process between an event's actual occurrence and the event time recorded by a hub varies depending on the wait times and back-off loop paths taken before a message is successfully transmitted.

The length of the inactive period, BI, PAN configurations, the length of the CFP, the number of sensors linked to the hub, and the amount of sensor traffic brought on by residents are all elements that affect the degree of delay caused during the communication. Multiple routers and various network topologies could make the procedure much more complicated and cause further delays, but they are not present in our design. If the channel is busy after receiving permission to use the CSMA/CA method, the transmission process

can be interrupted and must repeat the same procedures again. The CSMA/CA algorithm's delays are calculated and described in the next section.

4.4.2 Delay Calculation

The PANs examined in this research are a star-shaped network with a single hub at its core and no other hubs or routers involved which creates the simplest topology available for any PAN network. In accordance with the concept of adopting default values in uncertain situations, it is also assume that there are no assigned GTS and that the CFP length is zero. Any message has a maximum of five transmission attempts, or four default back-offs, after which it is deemed unsuccessful and deleted. If the channel is busy, the sensor backs off and waits a random period of time before making a second attempt, as shown in Figure 4.6. Back-off Exponent (BE), whose value varies with each attempt, is used to determine the length of time to wait between each attempt. Eq. 4.1 represents the formula to determine wait time in unit called backoff period using BE, where one backoff period when calculated according to the assumptions stated below table 4.2, would be equal to 1.025 msec.

$$t=Random(2^{BE-1}) = I*(2^{BE-1}) \quad (4.1)$$

where $I \in \{1,2\}$

The Battery Life Extension (BLE) variable determines the value of BE in slotted CSMA/CA; if BLE is set to 1, the sensor waits for a shorter period of time to prolong battery life. Table 4.2 summarizes the estimated latency for slotted and unslotted algorithms as a function of the required number of back-offs and the amount of the random delays. Additionally, waiting for a new slot boundary before beginning the process, which changes depending on the situation, waiting for the next beacon if there is less than one

IFS of CAP time remaining, and various random delays induced by waiting for the next beacon are all examples of delays produced by slotted CSMA/CA.

Table 4.2 Delay Estimates induced by both CSMA/CA technique based on number of back off(s) © 2021 IEEE

No. of Back-off(s)	Slotted CSMA/CA				Unslotted CSMA/CA	
	<i>BLE=0</i>		<i>BLE=1</i>		<i>BE</i>	<i>Delay (msec)</i>
	<i>BE</i>	<i>Delay (msec)</i>	<i>BE</i>	<i>Delay (msec)</i>		
0	3	7.2 – 8.1	2	3.1 – 4.0	3	7.2
1	4	22.5 – 23.5	3	10.3 – 11.2	4	22.5
2	5	54.1 – 55.1	4	25.6 – 26.6	5	54.1
3	5	85.8 – 86.8	5	57.2 – 58.2	5	85.8
4	5	117.4 – 118.5	5	88.9 – 89.9	5	117.4

a) For MSK PHY with a data rate of 2000 kb/s (IEEE standard default)

b) $\text{Random}(x)=1 \times x$ (minimum)

c) BI = 15.38 ms (minimum)

Additionally, the number of CCAs that must be done increases and fluctuates with each back-off; for these reasons, the delay for the slotted CSMA/CA is presented as a range. Unslotted CSMA/CA, on the other hand, does not have the concept of waiting for the next slot because there is no periodic beacon as CCA is always executed once in every attempt which allows us to estimate a single delay value. The possible range of packet transmission delays, which might affect how accurately the hub assigns time stamps, is shown in Table 4.2. The estimations in Table 4.2 were produced using a number of assumptions that were either listed in the text or briefly discussed below the table. For the purpose of determining a cautious estimate, these assumptions choose each at its minimal value and IEEE Std. 802.15-4 default values if they are defined. The delay variability will therefore increase if any of these values are changed from the selected values. Increasing the minimum random

delay, having a PAN with more than one hub/router, a more complex topology or simply more connected devices, or having competition for the real spectrum since Zigbee employs a frequency spectrum that is comparable to that of Wi-Fi and many other household wireless protocols—are further scenarios that will widen the range of delays.

4.5 Conclusion

This research has demonstrated that even under ideal circumstances, there are constraints on the time stamp precision for Zigbee sensor events that can cause concerns in the accuracy of any time sensitive calculations and even alter the order of sensor events making the data useless at times. The precise time stamp assigned to a sensor event in many applications may always be behind actual time and this difference will only be higher in real life than the estimates shown in the chapter. This research has demonstrated that the fundamental Zigbee protocol can introduce delays of up to 100 msec even under perfect circumstances. When comparing the relative times of two events, this delay will turn into a variable error. This inaccuracy will have a big impact on the computed difference when there isn't much actual time between the events. As a result, while integrating Zigbee sensors, the delay caused by the Zigbee protocol must be taken into account as a significant source of noise. These conclusions made it evident that aligned Zigbee operated motion sensors are not a wise choice for gait speed estimation thence birthing the need to an effective alternative. After exploring many of the existing alternatives and some promising counter products, the one found most effective is explored in the following chapters.

Chapter 5: Walking Gait Speed Measurement Using Privacy

Respecting AI Enabled Visual Sensor

Many of the existing options explored in Chapter 2 are either incapable of daily home monitoring and are dependent on lab setups; or are simple wearable and obtrusive in nature which contradicts the aim of this thesis. Video based assessment can resolve these issues as it provides regular rich data to work with and subjects do not need to remember to wear them regularly. Several works have been conducted on usage of regular RGB cameras or RGB depth camera for analysis of both gait speed and parameters like stride length. But this rich camera data comes at the cost of privacy of the residents of the house, which may cause them discomfort and limit the practicality of installing these cameras. Therefore, this chapter is introducing a novel privacy respecting camera by AltumView Systems Inc., currently available in market and is capable of fall event assessment. The experiments conducted in this chapter are aimed to extend its usage for gait speed estimation.

5.1 AltumView Sentinare Activity Visual Sensor

A video of a resident's everyday activities in their home has a wealth of information that can be utilized for numerous clinical evaluations as well as an accurate assessment of gait speed and other gait metrics. However, at the same time, it prompts questions about citizens' right to privacy, rendering them useless in practical situations. This thesis offers an AI-equipped visual sensor to address this problem. This is named as such since it is technically not a camera as it does not output an actual image or video but one of its components is a camera. The term camera and visual sensor are used interchangeably in the following contents of this thesis. Sentinare, an activity sensor powered by artificial

intelligence (AI) and created by AltumView Systems Inc., has the ability to run sophisticated algorithms to recognize human beings in video. This function enables the AltumView Sentinare sensor to output no actual video but the coordinates for 18 body parts including feet, knees, hands, elbows, shoulders, head, etc., instead of regular video frames. In order to accomplish that, Altumview visual sensor utilizes numerous complex algorithms such as face detection, joint detection, and so on. Using these points, a stick figure of the individual can then drawn over a still background image that has been previously taken and this image remains the same for each video frame. Now, it is possible to monitor residents' actions without compromising their privacy by using the sequence of these images. The collected data can be examined and used for gathering statistics, monitoring resident activity levels, and issuing alarms when mishaps like falls are discovered. Based on the stick figure data from the AltumView Sentinare sensor, a gait speed estimation algorithm will be designed in the following chapters. The visual sensor is also equipped with APIs to output the stick figure data for third-party integration, which is how it is being used for the research conducted during this thesis.

5.1.1 Experiment Setup

The setup is designed around 3 markers placed at consecutive distance of 1.828 m (6 ft) each to provide a consistent visual reference for the researchers. The AltumView sensor is placed at a perpendicular line intersecting the markers in middle as shown in Fig.5.1 (a) and Fig.5.2 The sensor must be placed so that it can see the full height of the subject for the AI to detect the subject body position and must also be able to see the full test distance for the gait assessment. The sensor height is set to be 1.32 m (4ft for stand height + 4in for sensor height) with the sensor aimed towards the floor with an angle of 10° from the

horizontal. This height allows a reduced sensor angle to the floor compared to a higher sensor position such as the manufacturer recommended 2 m for fall detection. When the sensor height was tested, it was discovered that when it was set to 2 m, the sensor had to be pointed down, which restricted the field of vision from including the subject as they entered the frame, failing to detect the subject. An illustration in Fig. 5.3 helps to understand this. This arrangement might be used to symbolize a camera mounted on a wall at the end of a hallway in a house.



Figure 5.1 (a) Lab setup (b) AltumView Sensor view of Lab setup with a sample stick figure © 2022

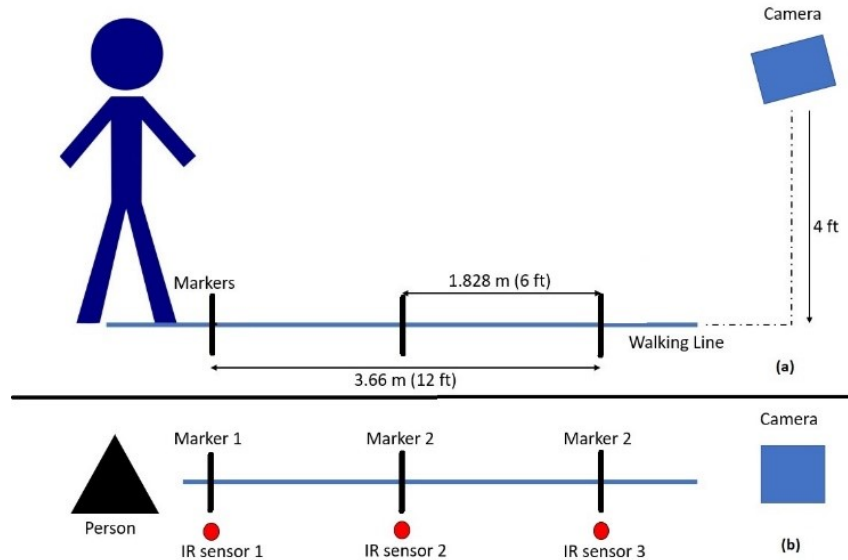


Figure 5.2 Illustration of lab setup (a) Side View (b) Top View © 2022 IEEE

Three IR break beam sensors are also installed with the sensor at a height of 1.23 m (4 ft), one on each marker. These sensors will measure the ground truth timing of the walks for later verification. The lab setup and sensor view of the lab are illustrated in Fig.5.1, while a sketch of the lab setup is presented in Fig.5.2 (a). Fig. 5.2 (b) represents the top view of the lab setup along with the IR sensor placement.

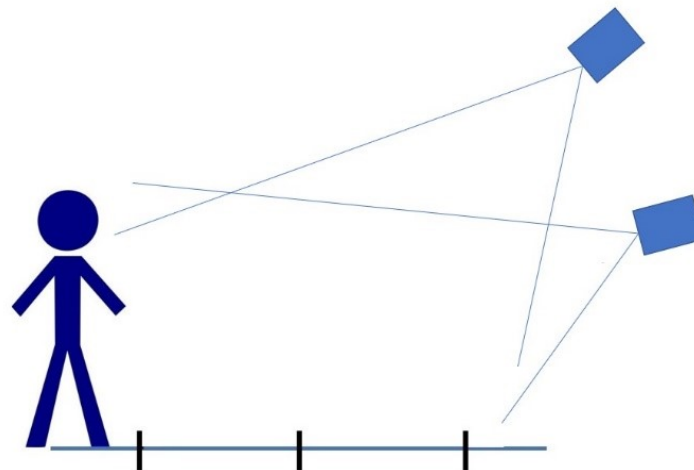


Figure 5.3 Illustration comparing field of view of camera at different heights © 2022 IEEE

3 IR break beam sensors are positioned beside the markers, each set to a height of 1.23 m to match the sensor's height and prevent early sensor tripping due to arm swinging

movements. These IR sensors are attached to an Arduino board, which continuously reads the sensors' states at a sampling rate of 115200 Hz and records the information in a local text file with millisecond-accurate timestamps. In order to extract the timestamps of the entries where IR sensors change their state from 0 to 1, where 0 represents no obstruction in the path of the IR beam and 1 signifies otherwise, these text files are then transformed into a csv file.

5.1.2 Data Acquisition

The collected image is processed by the AltumView sensor for each frame in order to determine the coordinates of 18 different points on the body of the individual in frame. These coordinates are transmitted to a local system as (8 header + 152*number of people in frame) 8-bit binary values via an API together with other significant data such as a person ID number, frame number, number of individuals in frame, etc. The 152 values for every individual are structured data that include the person's ID number, if available, and the coordinates for each of the 18 points in the stick figure. Since there is just one subject in the experiment described in this work, it can be assumed that the AltumView sensor transmits 160 8-bit binary values for each frame, which will be referred as the frame info in following contents of this thesis.

Not each of the frames captured by the internal camera is a candidate for application of the on-sensor AI algorithms since the AltumView sensor captures an internal 30 frames per second standard video stream that is promptly subsampled to 10 frames per second in order to reduce the computational load. Currently, real-time processing of every frame even at the 10 frame per second rate is not possible within the system due to the sensor's internal processing capability, and a frame's actual processing time varies. As a result, the sensor

does not process every frame and discards any that it is unable to process. The output frame rate from the sensor is a subset of the 10fps frames averaging around ~7-8 fps and sometimes goes as low as 3fps, reasons of which are discussed later in this chapter. The result is a signal with a synchronous sampling rate with many missing samples. The sensor output includes a frame number that allows for the location and number of missed frames to be identified.

A timestamp was attached by the local system as soon as it receives frame information communicated by the sensor which can be used for mapping of walks detected by sensor to walks detected by IR sensors during the verification process.

All of the frame information received from the sensor is combined into a log file, which is then processed to save the data in tabular form and refactor the normalized coordinates by multiplying them with background image dimensions. Extracted from the frame information, important details like timestamps, frame numbers, and ankle coordinates are saved in separate rows of the table, each column of which corresponds to a single frame.

5.1.3 Verification

The usage of IR break beam sensors to provide the ground truth timestamp values has been explained in the previous section. Having obtained the timestamps and hence the time taken to walk the pre-known distance, ground truth for gait speed can be calculated using the basic speed formula.

Since the data set had many consecutive walks each with different timings, the next important step for verification is to map each walk recorded by sensor to its ground truth recorded by IR sensors. This is attained using the timestamps attached to frame info received by the local system using the APIs as mentioned earlier. Timestamps for the frame when

ankles enter the 3.66 m walk line are compared to timestamps of IR instances when person enters the same. Since there is difference in timing when the IR sensors attach the time stamp and when the local system receiving the visual sensors' frame info attaches the time stamps, they are not necessarily exactly the same. Therefore, the walks with close time stamps are matched with each other. The following section elaborates on how the data collected using these setups is used to develop algorithms for precise gait speed assessment.

5.2 Methodology

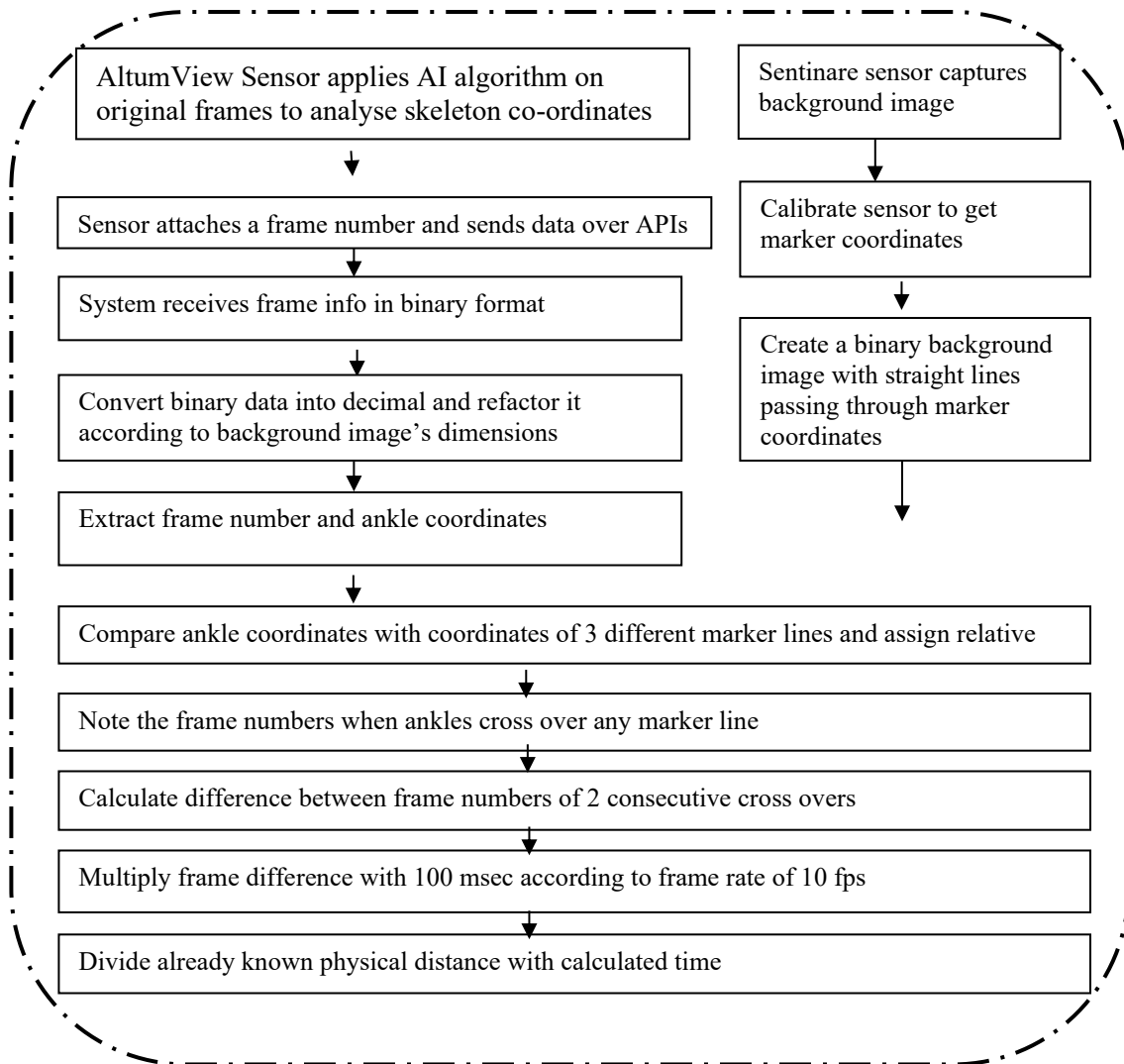


Figure 5.4 Flow Chart Explaining methodology

5.2.1 Sensor Calibration

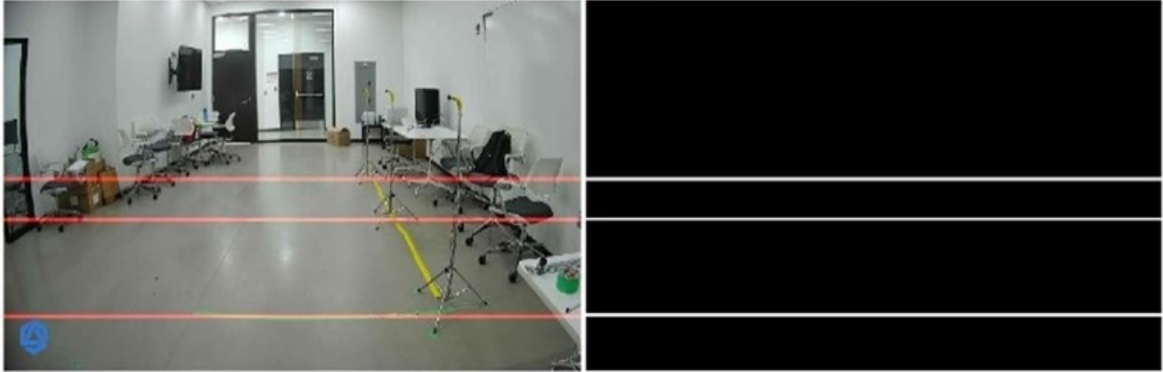


Figure 5.5 (a) Background Image with calibrated markers (b) Binary image created after calibration

© 2022 IEEE

The flow chart in Fig. 5.4 provides a concise explanation of the entire gait speed calculating process proposed in this chapter. The methodology is concentrated on measuring the amount of time needed to travel a specific distance as captured by the Sentinare sensor. As a result, it becomes necessary to establish references that are situated at a specific physical distance from one another. This is accomplished through sensor calibration, in which the floor is marked with three markers that create two successive distances of 1.828 m using green painter's tape, as shown in Fig. 5.5(a) for researcher reference. The individual stands on each marker with both feet apart, and the camera algorithm determines the coordinates of each foot without the direct need of the markers for calibration. The researchers can use the markers as a visual reference, but the calibration for the processing of Altumview data is based on where the feet are during calibration, not the marks themselves. The joint detection algorithm of the sensor uses the ankle coordinates from 50 consecutive frames of recorded data to locate the marker and minimise measurement variation error. The

equivalent markers on the background image are then created by drawing a straight line through the two points, as shown in Fig. 5.5 (b).

5.2.2 Relative Location Estimation

The methodology suggested in this chapter's primary premise is to record the amount of time needed to walk between any two visual markers, in other words to estimate time between crossover of any two visual markers. To do it, it's crucial to know the relative positions of both ankles in relation to each marker for all frames. The frames where both ankles could not be detected by the algorithms are discarded while processing the frame info messages. After this process, in some cases the number of usable frames was reduced to as low as 3 fps just like it was inferred earlier.

Because the AI program could only identify one of the ankles for some frames, an additional data processing step was added. Just like frames with ankle co-ordinates missing were deleted, dropping these frames also would result in the loss of extra crucial information, and it might even result in the merging of two successive walks. The "missing" relative locations for ankles are filled with the location of the second detected ankle in such frames since it is assumed that both feet are in the same relative location.

To do this, the coordinates of the virtual calibration lines as shown in the background image in Fig. 5.6 and divided into three separate variables, each of which stands for marker 1, marker 2, and marker 3, respectively.

For a single frame, a stick figure's ankle is actually just a pixel with a row and column number. The relative location is then calculated by comparing the location of that ankle pixel with the locations of markers 1, 2, and 3. This estimates a relative location, which is

subsequently recorded in a table. The illustration in Fig. 5.6 explains the estimation process and relative location format.



Figure 5.6 Diagram representing Relative location estimation © 2022 IEEE

5.2.3 Gait Estimation

Capturing the frames when ankles cross any markers is the next step after determining the relative placement of ankles in each frame. Based on the image sections created through virtual reference lines, the algorithm determines where each foot is located in relation to the calibrated markers. The frame numbers where each foot changes sections and crosses marker lines were then recorded. It should be noted that both feet may not enter or exit a section in the same frame; in such circumstances, there may be 2 consecutive “Entry” or “Exit” present. In these situations, computations are made using the frame number of the initial “Entry” or “Exit.”

The frame difference between the consecutive entrance and exit crossovers is computed when the frame numbers for the frames where ankles cross the markers are retrieved. Since the frame rate for the AltumView sensor is 10 fps, the frame difference is then multiplied

by 100 msec. The calculated time is then divided by the known distance, either 1.83m or 3.66m, to determine the gait speed.

5.3 Results

10 “Slow,” 10 “Average,” and 10 “Fast” walks along the walking line in each of the two potential directions were conducted in a controlled experiment. These walks were captured using IR break beam and AltumView Sentinare sensors, and the collected data was processed to determine the gait speed. The average walking speed determined by the sensors for each of the three groups is shown in Table 5.1 along with the observed mean error. The average speed recorded by the IR sensors is applied to determine the percentage error, with the IR sensors serving as the source of the ground truth values. As the feet were not detected in some of the frames, it was found from the outcomes that 10% of the total gait speed observations were incorrectly detected by the AltumView sensor due to missing “Entry” or “Exit” frames. These outliers were not included in the calculation of the average error.

Table 5.1 Average Error in Gait Speed © 2022 IEEE

Walk Type	Mean Gait Speed (m/sec)	Absolute Error (m/sec)	Standard Deviation	Percentage Error
Slow	0.852	0.118	0.084	14.3
Normal	0.971	0.136	0.152	13.2
Fast	1.780	0.203	0.202	12.7

Despite the missing frames, extremely low and asynchronous frame rate, and other restrictions, the sensor data demonstrates the potential of the suggested method by allowing

the estimation of walking speed with an average percentage error of 13–14%. The next section discusses the sensor’s shortcomings as they were discovered during the process, along with any potential fixes that might lower the mean error in the future.

5.4 Discussion

1	'19:40:55.1...	'19:40:55.3...	'19:40:55.7...	'19:40:57.4...	'19:42:38.5...	'19:42:38.7...
2	38927120	38927121	38927126	38927155	38928797	38928798
3	4.2950e+09	4.2950e+09	4.2950e+09	4.2950e+09	4.2950e+09	4.2950e+09
4	[656,229]	[656,229]	[656,229]	[656,229]	[638,217]	[638,217]
5	[661,229]	[656,229]	[661,229]	[0,0]	[644,217]	[644,217]
6	1x160 cell	1x160 cell	1x160 cell	1x160 cell	1x160 cell	1x160 cell

Figure 5.7 Screenshot of the processed data (1) Time stamp (2) Frame number (3) Person ID (4) Right Ankle coordinates (5) Left Ankle coordinates (6) All body coordinates © 2022 IEEE

The frame numbers listed in row 2 are not consecutive, as can be seen in Fig. 5.7, which is a screenshot of the tabular form of all the processed frame information. The missing frame numbers were either never transmitted to the local system or were removed because the AltumView algorithm was unable to detect ankle coordinates in them. Due to the on-sensor processing burden, it was necessary to remove the frames that were not conveyed, whereas AI algorithm limitations led to the loss of frames that missed ankle coordinates. In either case, the amount of time it takes to walk will be significantly increased or decreased if a frame is missing at the moment someone crosses a marker. In fact, it was found that this was the case with the exceptions indicated in the previous section.

The second and most important issue with the observed error is the low and asynchronous frame rate, which goes hand in hand with the issue of missing frames. The timestamps captured by IR sensors and the AltumView sensor as soon as the person enters the walking line for some randomly selected sample walks are represented by the values in columns 1

and 2 of Table 5.2. The difference in their timestamps is displayed in column 3 of the table once each walk has been mapped to its corresponding counterpart. The local system assigns the sensor timestamps after receiving the frame information, as was covered in earlier sections. The difference between them will indicate how long it took to process the frame and send the frame's information to the local system if the IR timestamp corresponds to the real moment the person entered the walking line. It is safe to assume that the majority of the difference and all of the variance is caused by the varied processing durations for each frame since in our experiment all frame information is 1280 bytes long and requires a very similar amount of time for transmission. The developers in AltumView also approved this hypothesis. With the foregoing information, it is safe to say that even though the camera of the Sentinare visual sensor has a synchronous sampling rate, the resulting frame rate is asynchronous with numerous missing samples.

Table 5.2 Difference in IR and Cam Time Stamps © 2022 IEEE

Cam Timestamp	IR Timestamp	Difference (sec)
'16:03:42.420'	'16:03:39.920'	2.500
'16:03:52.344'	'16:03:51.184'	1.160
'16:04:04.880'	'16:04:02.561'	2.319
'16:04:13.848'	'16:04:12.196'	1.652
'16:04:36.185'	'16:04:34.917'	1.268
'16:04:48.383'	'16:04:46.173'	2.210
'16:04:57.933'	'16:04:56.489'	1.444
'16:05:11.847'	'16:05:09.650'	2.197

Due to the involvement of these variables, it was decided against using the time received for a frame from the sensor because it will create some inaccuracies due to the variable processing time and frame numbers were used instead. The frame numbers increase at a

constant rate of 1 frame every 0.1 sec. This consistency allows us to accurately estimate the time taken with a margin error of ± 50 msec. If the algorithm used by the AltumView sensor is changed to provide a timestamp attached to a frame when it is collected, this margin error can reduce significantly, greatly improving the accuracy of the ensuing gait analysis.

The observed inaccuracy can be attributed to the interaction between the asynchronous frame rate and the generally low frame rate for the AI processed data. As previously stated, the 10fps sensor video is processed for about one out of every three frames. There is no way to guarantee that the real cross over did not take place in one of the missing frames because the methodology heavily depends on the frame where the person “crossed” the marker. The performance of the embedded system will improve with microprocessor advancements, and it may be able to increase the number of frames that can be processed, resulting in a higher frame rate and better accuracy. However, it might not be too soon before technology reaches that level. The following chapter, which addresses the urgent need, suggests an algorithm that can partially compensate for the lack of hardware technology and makes an attempt to address these problems.

Chapter 6: Method to Improve Gait Speed Assessment for Low Frame Rate AI Enabled Visual Sensor

In previous chapter, a basic approach for gait assessment highlighting the potential of an innovative visual sensor was designed. AltumView (Altumview Inc, Burnaby, BC) Sentinare activity sensors use AI to extract body parts in real time and generate skeleton stick figures based on those coordinates. These skeleton stick figures are mapped over a pre-captured background image, thus addressing the privacy concerns associated with using cameras. Chapter 5 explained an algorithm to operate the visual sensor, however the asynchronous and low frame rate of the sensor raised concerns and limitations.

The algorithm listed in this chapter explores a way to rectify this issue by regenerating lost frame data with frame rates as low as 3 frames per second back to the standard camera frame rate of 30 frames per second. An algorithm that uses regression to regenerate missing data is introduced in this chapter. The bisection method is then applied to the regressed polynomials to estimate gait speed. An erudite comparison is also provided in this chapter on the performance of the proposed algorithm based on the chosen regression degree of freedom.

6.1 Methodology

The detailed discussion on results obtained from the previous algorithm is available in Chapter 5 but one of the major take-aways was the fact that low and asynchronous frame rate of the Altumview visual sensor is one of the key reasons behind the observed error. We discussed in previous chapter how Altumview sensor first reduces the frame rate to 10 which is further reduced to $\sim 7-8$ fps due to technical issues. It was also discussed that this rate

occasionally drops to 3 fps when the visual sensor is no able to detect ankle properly in the captured video and how this may result in uncertainty if the “entry” frame detected by previously proposed algorithm is the actual entry frame or simply one of the consecutive ones. Same reasoning is applicable on the exit frames which results in unwanted addition or subtraction of time to the original time taken for the walk. Hence, all in all this establishes the importance of the lost data and how recovering it can improve our accuracy.

Therefore, this chapter proposes a data estimation algorithm which attempts to estimate the ankle point coordinates in the lost frames and restore the frame rate back to 30 frames per second. Followed by data estimation, same idea of calculating time taken to walk a known distance is used to calculate the walking speed of the subjects.

The methodology proposed in this chapter requires the AI camera to be calibrated using markers to indicate the position of the walking line virtually in the background image, just as explained in the previous chapter. The calibration steps used here were also explained in detail in the previous chapter.

6.1.1 Walk Data Overview

The proposed algorithm initiates by understanding the original data transmitted from the Altumview sensor, better which is achieved by plotting the x coordinate and y coordinate of both right and left leg against their frame numbers. These plots are shown in Figure 6.1, which contains the data for 10 consecutive walks in opposite directions at “Normal” pace. As the walk line aligns vertically along with columns of the background image, the y-coordinates represent the position of the subject on the walk line. It can be seen in the experiment setup shown in Figure 5.1 that the camera is located towards the bottom of the background image, hence whenever the subjects walk towards the camera, the value of the

y coordinate goes up and vice-versa. This pattern is clearly visible in the plots shown in Figure 6.1. Moreover, following this pattern the 10 walks mentioned can easily be distinguished from each other in the plots. Another noticeable pattern visible in the plots is the co-ordinates going zero periodically. According to the camera specifications, 0 value of co-ordinates represent that the said body part is not in the frame. The attempted walk was indeed carried out in a manner that the subjects walk out of the frame as they come closer to the camera. This justifies the zero values of co-ordinates when it reaches its peak.

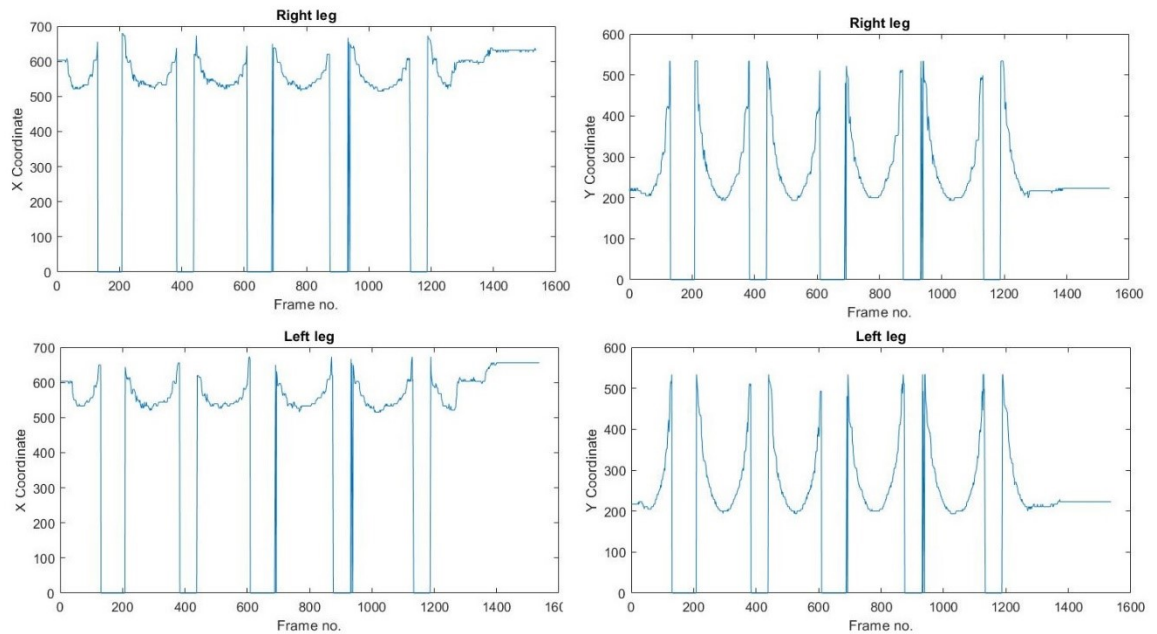


Figure 6.1 Graph of x-y coordinates of both ankles versus the frame number

6.1.2 Peak and Valley Location

It can be observed in the plots of Figure 6.1 that each separate walk follows a certain underlying pattern which can be potentially exploited to fill in the missing data. In order to understand this underlying pattern better, it is needed to understand the geometric patterns which occur when a 3-D world is captured in a 2-D image by the camera. A same distance

in the physical world would appear shorter in the image if placed farther away from the camera however it appears larger if placed near to the camera. Following this pattern, it can be concluded that the changes in values of vertical co-ordinates are smaller when the subject is walking far from the camera, and it gradually increases as the subject move towards the camera. This same pattern is exhibited in the plots of Figure 6.1 which makes the data for a walk at constant speed to appear as an upward curve in the plots. After it is established that all the theories are indeed visible in our recorded data without any anomalies, the next step requires to estimate the dynamics of these curves so that missing values can be estimated. So as to achieve that, first it is required to roughly separate each walk from the combined data which in our case is accomplished by manually marking all the peaks and valleys in the plot thence isolating all the walks from each other.

6.1.3 Curve Fitting and Data Estimation

After the isolation, now it is possible to estimate the coefficients of the underlying curve in each walk with the help of curve-fitting which defines the next step in our algorithm. However, before performing curve-fitting, the frames where ankle coordinates were not detected i.e., the frames with 0 co-ordinate value which acted as outliers were deleted to clean the data. In order to study the performance of different regression degrees of freedom, linear, quadratic, and cubic regression was performed on the extracted data. To normalize the data, the first frame number was reduced to zero by subtracting it from all the frame numbers before performing the regression. When the data were regenerated, this number was then added back in.

Using the polynomials obtained following regression, data can be restored to 30 frames/sec after curve fitting. While the data were regenerated, frame numbers assigned to the

regenerated data were not integers due to the 10 frames/sec rate assumed by the camera and replacement frames were essentially assigned between the existing 10 frames/sec integer frames. In this way, the frame number pattern of 0, 1, 2... has been enhanced to 0, 0.33, 0.67, 1, 1.33... and so on. Figure 6.2 shows the plots created after y co-ordinate data for both right and left ankles was regenerated using all the estimated polynomial coefficients.

6.1.4 Gait Speed Estimation

Post data restoration, the subsequent step required in the algorithm is to estimate number of frames taken to walk a pre-known distance which follows the same idea as the previously proposed algorithm in Chapter 5. As a consequence, the algorithm starts with calibrating the camera to draw virtual markers of the walk line on the background image using the steps explained in section 5.2.1. The only difference in this process is that moving forward, instead of using few rows wide marker, the value of mid row of the marker is used for the calculations. Unlike the previously proposed algorithms, instead of tracking the frame when ankle co-ordinate values exceed the marker line co-ordinates, the inverse ideology is utilised for creating the algorithm to get better perfection. Numerical methods were used to track the frame number when the ankle co-ordinate is equated to the marker co-ordinate. The objective here is to figure out what value of frame number, does the regressed polynomial equation match with the marker co-ordinates. The $h(f)$ depicted in equation (6.1) represents the calculated row number for a given frame number (f) i.e. it represents the polynomial obtained in section 6.1.3. In an attempt to find out when the ankles exactly step over the virtual marker lines and hence the ankle co-ordinates ($h(f)$) overlap with the marker co-ordinates (r_{mi}), equation (6.2) must be satisfied where r_{mi} represents the row number for each marker line. Equation (6.2) can be reformed into equation (6.3) allowing the bisection

numerical method to be used to calculate the root of equation (6.3) which is the desired frame number for the ankle crossing each line.

$$h(f) = a_n f^{n-1} + a_{n-1} f^{n-2} + \dots + a_0 \quad (6.1)$$

$$h(f) = r_{mi} \quad i = 1, 2 \quad (6.2)$$

$$g(f) = h(f) - r_{mi} = 0 \quad (6.3)$$

Given the fact that the frame numbers were assigned based on a frame rate (f) of 10 fps rate, frame difference of 1 corresponds to 100 msec and frame difference of 0.33 corresponds to 33.33 msec, thence the frame count difference enables estimation of the time interval between the crossing of markers. The fractional values of frame numbers obtained from equation 6.3 were rounded off to the frame number pattern explained in section 6.1.3 in order to stay true to 30 fps frame rate. The gait speed is computed by dividing the known distance between the markers by the projected time. Depending on which ankle crossed the marker first, the data from the right and left ankles were merged for these calculations and were also utilised independently to calculate gait speed. The time necessary between the first ankle crossing each line—which could be left, right, or one of each—is used to determine the gait speed for the combined findings.

6.2 Results

Table 6.1 Root Mean Square Error (in pixels) © 2022 IEEE

Ankle	Linear	Quadratic	Cubic
Right (x)	119	63	53
Right (y)	305	134	109

Left (x)	118	67	57
Left (y)	288	109	79

The accuracy of the regression fit is shown in Table 6.1 for the right and left ankle x-y coordinates using the root mean squared error calculated from the linear, quadratic, and cubic regression models.

30 walks were tracked during the trial, including 10 "Slow," 10 "Normal," and 10 "Fast" walks. The subject's walking speed was estimated individually using information from the Sentinare visual and IR sensors. The algorithm presented in Chapter 5 directly determined gait speed at a low frame rate. By displaying the mean absolute error and mean percentage error, Table 6.2 compares these outcomes to the updated methodology suggested in this chapter.

Even if it is assumed that the person is moving along at a constant speed, the results shown in Table 6.2 demonstrate how poorly the linear regression fit performs. This demonstrates that the distance travelled in pixels over a predetermined number of frames does not correspond to the distance travelled over a predetermined length of time on the ground. It can be accounted for by the distortions brought on by the camera's 3D to 2D mapping. The cubic regression fit is clearly more accurate than the quadratic fit, however it's important to note that the quadratic regression gait assessment outperforms the cubic regression measure (see Table 6.1). Except for when the subject is further away from the camera, the cubic and quadratic curves are very similar to one another, as shown in Fig. 6.2 and expanded in Fig. 6.3 to show the detail. The estimated gait speed from the cubic and quadratic polynomials for walking away from the camera in Fig. 6.3 differs significantly because of this. The results, which indicate that the quadratic fit works better, are summarised in Table 6.2.

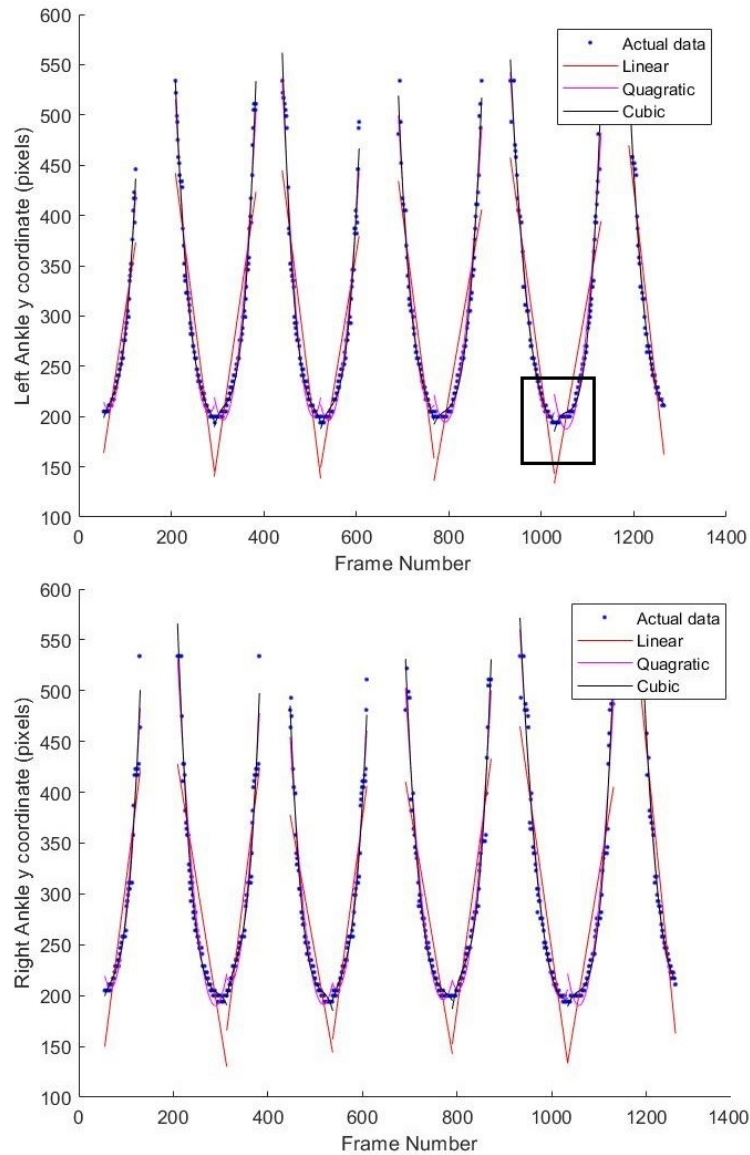


Figure 6.2 Graph representing the estimated y coordinates versus frame data for both ankles, by all three regressed polynomials. The region shown in the black box is enlarged in Figure 6.3 © 2022 IEEE.

Another intriguing discovery is that, despite the percentage error remaining constant from the previous results, the absolute error standard deviation has dropped significantly. In contrast to the previous case, which had varying numbers of frames accessible at various times, this illustrates the consistency of the suggested strategy because each walk scenario now had the same number of frames available.

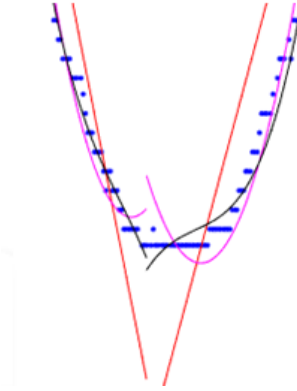


Figure 6.3 Example enlargement showing the difference between the regression curves for the quadratic, cubic and linear polynomial when the subject ankles are close the camera. This is an enlargement of the region shown in Figure 6.2 © 2022 IEEE.

The left ankle's performance parameters are noticeably different from the right ankle's, however they are quite similar to the performance parameter derived from the combined data from both ankles. According to which ankle crossed each marker first, the data from the right and left ankles were combined. The left ankle crossed the marker lines first most frequently as observed during the combining procedure, which explains why the combined data and the left ankle data produced comparable results. Additionally, it should be noted that right ankle data performs noticeably better than left ankle data.

Table 6.2 Average error of gait speed estimation © 2022 IEEE

Error Type	Previous Results	Right			Left			Combined		
		Linear	Quadratic	Cubic	Linear	Quadratic	Cubic	Linear	Quadratic	Cubic
Avg. Absolute Error (m/sec)	0.14	0.42	0.06	0.11	0.41	0.11	0.14	0.41	0.11	0.14
Std. Deviation of Absolute Error (m/sec)	0.15	0.14	0.04	0.07	0.16	0.07	0.09	0.16	0.06	0.09
Avg. Percentage Error (%)	13.2	41.1	6.3	10.6	40.0	10.9	13.8	40.0	10.7	13.8

6.3 Discussion

The solution suggested in this research effectively regenerates the data which was lost as a result of the Sentinare vision sensor's significant processing load that limits the frame rate. As a result, there are better foundations for an accurate calculation of gait speed. This enables the estimate of the ankle position to be restored to the frame rate of 30 frames/sec. The results from the preceding chapter are improved by as much as 7% when the gait speed is calculated using the suggested method. Even though the performance of the right and left ankles differs greatly, Sentinare visual sensor has a wide range of applications and can be used to track other body parts in the future instead of the ankles to improve the results.

The performance disparity between the left and right leg findings in relation to the IR sensor has to be further examined. In contrast to the suggested technique, which tracks ankle movement, the ground truth data is gathered using infrared break beam sensors placed at a height of 4 feet and tracks torso movement. While walking, our body maintains a more constant motion while our feet alternate between periods of movement and immobility. It is reasonable to suppose, given the experimental setup, that there are a few milliseconds between the initial step (in this case, the left ankle crossing the marker) and the torso crossing the break beam sensor. Similar to that, there is a lag between the second step and the torso crossing over (i.e., in our case right ankle). These variations are not consistent, possibly due to factors like uneven stride lengths, which results in a variation in the time recorded to walk the gait line distance.

Chapter 7: Conclusion and Future Work

7.1 Thesis Conclusion

The main objective of the thesis is to estimate walking speed of the residents of a smart home using some unobtrusive sensor networks. A series of five experiments were conducted, each building on top of the conclusion from the previous one trying to overcome its limitations. Some new algorithms were developed during the process and successively updated resulting in the major contributions of the thesis. These contributions include showing a connection between gait movements and cognitive abilities of older adults, highlighting the major limitations of wireless protocols like Zigbee for time sensitive measurements, and introduction to vast capabilities of an AI enabled visual sensor.

Using motion sensors deployed within individuals' homes, the first experiment of this thesis established that longitudinal data could be collected on gait and activity levels through technology. Mild cognitive impairments were observed to have different activity levels than normal cognitively functioning individuals. Gait line detection of the mean number of daily walking events was significantly higher for CDR 0 participants (101.4) than for CDR 0.5 participants (92.8).

Due to some observations made during first experiment, the second set of experiments was conducted using two sets of motion sensors. Even when conditions are near-optimal, Zigbee sensor events' time stamp precision can still be affected, resulting in variable time stamp accuracy and even modifying the order of sensor events. The results from this study demonstrate that Zigbee can introduce delays of more than 100 msec, even under ideal circumstances. When two events are in the same relative time frame, this delay becomes a

variable error. The Zigbee protocol-induced delay must therefore be taken into account as a noise factor when using Zigbee sensors. Due to the model's exclusion of many other sources of variance and the assumption of conservative Zigbee protocol parameters, the actual variation can be higher than predicted. This model provided the explanation for the observed large variance in the measured time stamps and predicted the observed order reversal for time stamps, given that different sensors might experience different contention back-offs.

After it was established that Zigbee operated motion sensors could no longer be used for gait speed estimation, the third experiment was conducted introducing a novel AI enabled visual sensor. The proposed methodology effectively calculates the walking speed of the residents for each walk without intruding into their privacy with the help of an intelligent sensor. The videos recorded by the sensor, despite having many shortcomings such as low and asynchronous frame rate, missing frame etc., provides rich data laying the foundation of the proposed method. The result of this experiment shows the potential of this alternative for assessing walking speed.

It was estimated that the error rate for the walks under study was between 13-14%, including the 10% of the cases where the camera did not record the entry or exit frames for a walk, most likely as a result of low frame rates. Due to the low frame rate used, the performance is much better than expected since cases where an exit event was missed due to the frame rate were excluded.

The sensor's processing capacity limits the performance, but as processor performance improves, higher AI frame rates and more precise gait estimation can be achieved. By

modifying the timestamp definition in the AltumView sensor, the gait analysis can be performed more accurately as well.

In order to improve the limitations of the third experiment, fourth experiment was conducted attempting to restore the frame rate of visual sensor. The methodology proposed for this experiment efficiently regenerates the data lost due to the heavy processing loads with the Sentinare visual sensor that limit the frame rate. This allows the estimate of the ankle position to be restored to the frame rate of 30 frames/sec, thus providing better grounds for accurate gait speed estimation. The gait speed calculated using the proposed method reduces the error percentage by as much as 7% improving on the results of the previous experiment.

All in all, the work performed in this thesis managed to establish the link between the declining health of older adults and their gait analysis thence establishing the importance of regular gait monitoring in elderly care. Smart homes are no doubt the best way to achieve that goal as frequent visits to doctors is not a feasible option. One major finding of this research was that superficially perfect looking battery saving sensors might seem like a good option for gait monitoring, but due to the rules of the underlying protocols future researchers should take certain things into consideration before designing an algorithm around them. Our work proposes an easy to install privacy respecting camera as the alternative which is supposed to be plugged in a socket solving the issue of battery life. The proposed camera communicates the data with any system wirelessly using APIs, which can be further used for gait speed estimation and more. Proposed algorithms in this thesis managed to achieve an accuracy of 93.7% in gait speed estimation relying on the current

technology, and our research showed that the potential of this device is vast, and accuracy will only improve with advancement in technology.

7.2 Thesis Contribution

This thesis has provided four main contributions while aiming towards the end goal of estimating gait speed in smart home setting unobtrusively. The first major contribution was the establishment of the fact that indeed walking activity can be linked with declining health conditions in older generation [13]. The second contribution was highlighting the unavoidable variable delay introduced by battery saving protocols like Zigbee, making sensors equipped with them unsuitable for time sensitive measurements [14]. The third contribution is made by proving the vast capabilities of an AI enabled visual sensor which at the same time overcomes the privacy issue induced by regular RGB cameras [15]. One of the major limitations of the AI enabled visual sensor i.e. low and asynchronous frame rate is addressed by the fourth contribution which is made by introducing regression based algorithm to restore the frame rate by estimating the values in missing frame [16].

7.3 Thesis Limitations

The limitations of the first set of sensors suggested in the thesis which is the motion sensors, is established over the development of the thesis. The second sensor which is a privacy respecting AI enabled visual sensor, introduced as a potential alternative to the existing sensors comes with its own set of limitations which are discussed in this section.

One of the major limitations of this visual sensor comes with the accuracy of all the algorithms it is embedded with. Although individually, the accuracy of all these algorithms like face detection, joint detection etc. is above 90%, but when practically implemented to

create the stick figure videos from the original regular RGB videos, it creates an ambiguity on the position of a certain body point in consecutive frames even if there is no movement. Another major limitation is the computation complexity of the algorithms and the lack of time and computation power required to execute those algorithms on every frame. Lack of timestamps on each frame content also becomes an issue due to this reason.

The performance of the proposed algorithm is limited by various reasons like accuracy of joint detection algorithm, accuracy of regression fit etc., however the most prominent limitation of proposed algorithm lies in its implementation in real world scenario where installation of a camera directly facing the walk line might not be possible.

7.4 Future Work

This work will require further exploration of the sensor including work to explore algorithm methods for different viewing angles between the sensor and the walking line as these will be required to address widely differing residential architectures. The potential for the sensor to be used in measuring other aspects of gait should also be explored such as stride length and pace. Future enhancement to the proposed algorithm with different known and unknown viewing angles between the sensor and the walking line. In addition to that, further potential of the device can be explored by tracing other body parts. Experiments including changing the camera height and its angle from the horizontal can be performed in order to achieve that. To improve the practicability of the visual sensor, an algorithm can also be developed where residents are not required to walk in straight line increasing the possibility to implement it in houses where a hallway is absent. The capability of the sensor to measure other aspects of gait will also be studied like stride length and pace. To explore the impact this may have on the clinical measurement of gait speed in a free living

environment, validation studies are needed that compare gait speed estimates from the sensor line to other precise methods of measuring gait speed that do not use the Zigbee protocol.

References

- [1] S. C. Government of Canada, “The Daily — Canada’s population estimates: Age and sex, July 1, 2019,” Sep. 30, 2019. <https://www150.statcan.gc.ca/n1/daily-quotidien/190930/dq190930a-eng.htm> (accessed Aug. 28, 2020).
- [2] “A Policy Framework to Guide a National Seniors Strategy for Canada,” p. 33.
- [3] P. Leung, M. Cheung, D. Kao, and A. C. Gulati, “Prevalence and predictors of depression in the older Asian Americans in Houston,” *Int. Soc. Work*, vol. 60, no. 4, pp. 800–814, Jul. 2017.
- [4] J. M. Haro *et al.*, “Analysis of burden in caregivers of people with Alzheimer’s disease using self-report and supervision hours,” *J. Nutr. Health Aging*, vol. 18, no. 7, pp. 677–684, Aug. 2014.
- [5] M. B. Lilly, C. A. Robinson, S. Holtzman, and J. L. Bottorff, “Can we move beyond burden and burnout to support the health and wellness of family caregivers to persons with dementia? Evidence from British Columbia, Canada: Supporting family caregivers in Canada,” *Health Soc. Care Community*, vol. 20, no. 1, pp. 103–112, Jan. 2012.
- [6] M. F. Winkler, V. M. Ross, U. Piamjariyakul, B. Gajewski, and C. E. Smith, “Technology Dependence in Home Care: Impact on Patients and Their Family Caregivers,” *Nutr. Clin. Pract.*, vol. 21, no. 6, pp. 544–556, 2006.
- [7] P. Topo, “Technology Studies to Meet the Needs of People With Dementia and Their Caregivers: A Literature Review,” *J. Appl. Gerontol.*, vol. 28, no. 1, pp. 5–37, Feb. 2009.

- [8] A. Clegg, J. Young, S. Iliffe, M. O. Rikkert, and K. Rockwood, “Frailty in elderly people,” *The Lancet*, vol. 381, no. 9868, pp. 752–762, Mar. 2013.
- [9] S. K. Inouye, S. Studenski, M. E. Tinetti, and G. A. Kuchel, “Geriatric Syndromes: Clinical, Research, and Policy Implications of a Core Geriatric Concept: (See Editorial Comments by Dr. William Hazzard on pp 794–796),” *J. Am. Geriatr. Soc.*, vol. 55, no. 5, pp. 780–791.
- [10] E. Viehweger *et al.*, “Influence of clinical and gait analysis experience on reliability of observational gait analysis (Edinburgh Gait Score Reliability),” *Ann. Phys. Rehabil. Med.*, vol. 53, no. 9, pp. 535–546, Nov. 2010.
- [11] “The State of Seniors Health Care in Canada,” p. 20.
- [12] G. Demiris, “Smart Homes and Ambient Assisted Living in an Aging Society,” *Methods Inf. Med.*, vol. 47, no. 01, pp. 56–57, 2008, doi: 10.1055/s-0038-1625127.
- [13] N. W. Thomas *et al.*, “Evaluating changes in gait and activity associated with cognitive impairment using a home-based technology platform,” *Alzheimers Dement.*, vol. 17, p. e056085, Dec. 2021.
- [14] A. Agarwal *et al.*, “Using Zigbee Sensors for Ambient Measurement of Human Gait – Analytical Considerations,” in *2021 IEEE International Symposium on Medical Measurements and Applications (MeMeA)*, 2021.
- [15] A. Agarwal, F. Knoefel, B. Wallace, N. Thomas, and R. Goubran, “Walking Gait Speed Measurement Using Privacy Respecting AI Enabled Visual Sensor,” in *2022 IEEE International Symposium on Medical Measurements and Applications (MeMeA)*, 2022.

- [16] A. Agarwal, F. Knoefel, B. Wallace, N. Thomas, and R. Goubran, "Method to Improve Gait Speed Assessment for Low Frame Rate AI Enabled Visual Sensor," in *IEEE 2022 Sensors Applications Symposium (SAS)*, 2022.
- [17] P. Holub, "Gait Analysis in the 19th Century: Motion Brought To Light," *Kindle Direct Publ.*, Oct. 2017, [Online]. Available: https://nsuworks.nova.edu/hpd_hs_facarticles/70
- [18] R. Baker, "The history of gait analysis before the advent of modern computers," *Gait Posture*, vol. 26, no. 3, pp. 331–342, Sep. 2007.
- [19] F. R. Marino *et al.*, "Gait Speed and Mood, Cognition, and Quality of Life in Older Adults With Atrial Fibrillation," *J. Am. Heart Assoc.*, vol. 8, no. 22, p. e013212, Nov. 2019.
- [20] K. S. van Schooten, M. Pijnappels, S. R. Lord, and J. H. van Dieën, "Quality of Daily-Life Gait: Novel Outcome for Trials that Focus on Balance, Mobility, and Falls," *Sensors*, vol. 19, no. 20, p. 4388, Oct. 2019.
- [21] S. Bridenbaugh, A. U. Monsch, and R. W. Kressig, "P1-073: How does gait change as cognitive decline progresses in the elderly?," *Alzheimers Dement.*, vol. 8, no. 4S_Part_4, pp. P131–P132, 2012.
- [22] L. di Biase *et al.*, "Gait Analysis in Parkinson's Disease: An Overview of the Most Accurate Markers for Diagnosis and Symptoms Monitoring," *Sensors*, vol. 20, no. 12, Art. no. 12, Jan. 2020.
- [23] M. L. Weidemann, K. Trentzsch, C. Torp, and T. Ziemssen, "Enhancing monitoring of disease progression-remote sensing in multiple sclerosis," *Nervenarzt*, vol. 90, no. 12, pp. 1239–1244, Dec. 2019.

- [24] S. A. Roelker, M. G. Bowden, S. A. Kautz, and R. R. Neptune, “Paretic propulsion as a measure of walking performance and functional motor recovery post-stroke: A review,” *Gait Posture*, vol. 68, pp. 6–14, Feb. 2019, doi: 10.1016/j.gaitpost.2018.10.027.
- [25] M. Kahya *et al.*, “Brain activity during dual task gait and balance in aging and age-related neurodegenerative conditions: A systematic review,” *Exp. Gerontol.*, vol. 128, p. 110756, Dec. 2019, doi: 10.1016/j.exger.2019.110756.
- [26] Keystone.Health, “Geriatric Diseases: Age-Related Medical Conditions & Illnesses.” <https://keystone.health/geriatric-diseases#:~:text=Many%20age%20related%20changes%20are,aging%20process%20for%20older%20adults>.
- [27] M. Rosselli and V. L. Torres, “Executive Dysfunction During Normal and Abnormal Aging,” in *Dysexecutive Syndromes: Clinical and Experimental Perspectives*, A. Ardila, S. Fatima, and M. Rosselli, Eds. Cham: Springer International Publishing, 2019, pp. 155–175. doi: 10.1007/978-3-030-25077-5_8.
- [28] “Telling The Difference Between Normal And Abnormal Aging.” <https://www.sunriseseniorliving.com/blog/january-2014/telling-the-difference-between-normal-and-abnormal-aging.aspx> (accessed Jun. 28, 2022).
- [29] “Healthy Aging,” *Memory and Aging Center*. <https://memory.ucsf.edu/symptoms/healthy-aging> (accessed Jun. 28, 2022).
- [30] A. Freedman and J. Nicolle, “Social isolation and loneliness: the new geriatric giants: Approach for primary care,” *Can. Fam. Physician*, vol. 66, no. 3, pp. 176–182, Mar. 2020.

- [31] A. H. Snijders, B. P. van de Warrenburg, N. Giladi, and B. R. Bloem, “Neurological gait disorders in elderly people: clinical approach and classification,” *Lancet Neurol.*, vol. 6, no. 1, pp. 63–74, Jan. 2007, doi: 10.1016/S1474-4422(06)70678-0.
- [32] B. R. Bloem, J. Haan, A. M. Lagaay, W. van Beek, A. R. Wintzen, and R. A. C. Roos, “Investigation of Gait in Elderly Subjects Over 88 Years of Age,” *Top. Geriatr.*, vol. 5, no. 2, pp. 78–84, Apr. 1992, doi: 10.1177/002383099200500204.
- [33] F. Onen, M. C. Henry-Feugeas, C. Roy, G. Baron, and P. Ravaud, “Mobility decline of unknown origin in mild cognitive impairment: An MRI-based clinical study of the pathogenesis,” *Brain Res.*, vol. 1222, pp. 79–86, Jul. 2008, doi: 10.1016/j.brainres.2008.05.027.
- [34] “Patient History and Dementia | Stanford Health Care.” <https://stanfordhealthcare.org/medical-conditions/brain-and-nerves/dementia/diagnosis/patient-history.html> (accessed Jun. 28, 2022).
- [35] R. Fukuda, Y. Shimizu, and N. Seto, “Issues experienced while administering care to patients with dementia in acute care hospitals: A study based on focus group interviews,” *Int. J. Qual. Stud. Health Well-Being*, vol. 10, p. 10.3402/qhw.v10.25828, Feb. 2015, doi: 10.3402/qhw.v10.25828.
- [36] E. Burleigh, I. Reeves, C. McAlpine, and J. Davie, “Can doctors predict patients’ abbreviated mental test scores,” *Age Ageing*, vol. 31, no. 4, pp. 303–306, Jul. 2002, doi: 10.1093/ageing/31.4.303.
- [37] D. M. J. Harwood, T. Hope, And R. Jacoby, “Cognitive impairment in medical inpatients. II: Do physicians miss cognitive impairment?,” *Age Ageing*, vol. 26, no. 1, pp. 37–39, Jan. 1997, doi: 10.1093/ageing/26.1.37.

- [38] S. E. Campbell *et al.*, “A multi-centre European study of factors affecting the discharge destination of older people admitted to hospital: analysis of in-hospital data from the ACMEplus project,” *Age Ageing*, vol. 34, no. 5, pp. 467–475, Sep. 2005, doi: 10.1093/ageing/afi141.
- [39] Z. S. Nasreddine *et al.*, “The Montreal Cognitive Assessment, MoCA: A Brief Screening Tool For Mild Cognitive Impairment,” *J. Am. Geriatr. Soc.*, vol. 53, no. 4, pp. 695–699, 2005, doi: <https://doi.org/10.1111/j.1532-5415.2005.53221.x>.
- [40] T. N. Tombaugh, “Trail Making Test A and B: Normative data stratified by age and education,” *Arch. Clin. Neuropsychol.*, vol. 19, no. 2, pp. 203–214, Mar. 2004, doi: 10.1016/S0887-6177(03)00039-8.
- [41] S. Jitapunkul, I. Pillay, And S. Ebrahim, “The Abbreviated Mental Test: Its Use and Validity,” *Age Ageing*, vol. 20, no. 5, pp. 332–336, Sep. 1991, doi: 10.1093/ageing/20.5.332.
- [42] H. M. Hodkinson, “Evaluation of a Mental Test Score for Assessment of Mental Impairment in the Elderly,” *Age Ageing*, vol. 1, no. 4, pp. 233–238, Nov. 1972, doi: 10.1093/ageing/1.4.233.
- [43] R. Katzman, T. Brown, P. Fuld, A. Peck, R. Schechter, and H. Schimmel, “Validation of a short Orientation-Memory-Concentration Test of cognitive impairment,” *Am. J. Psychiatry*, vol. 140, no. 6, pp. 734–739, 1983, doi: 10.1176/ajp.140.6.734.
- [44] B. J. Mainland and K. I. Shulman, “Clock Drawing Test,” in *Cognitive Screening Instruments: A Practical Approach*, A. J. Larner, Ed. Cham: Springer International Publishing, 2017, pp. 67–108. doi: 10.1007/978-3-319-44775-9_5.

- [45] S. Borson, J. Scanlan, M. Brush, P. Vitaliano, and A. Dokmak, "The Mini-Cog: a cognitive 'vital signs' measure for dementia screening in multi-lingual elderly," *Int. J. Geriatr. Psychiatry*, vol. 15, no. 11, pp. 1021–1027, 2000.
- [46] H. Brodaty *et al.*, "The GPCOG: A New Screening Test for Dementia Designed for General Practice," *J. Am. Geriatr. Soc.*, vol. 50, no. 3, pp. 530–534, 2002.
- [47] L. Berg, "Clinical Dementia Rating," *Br. J. Psychiatry*, vol. 145, no. 3, pp. 339–339, Sep. 1984, doi: 10.1192/S0007125000118082.
- [48] G. R. Cutter, "Development of a multiple sclerosis functional composite as a clinical trial outcome measure," *Brain*, vol. 122, no. 5, pp. 871–882, May 1999, doi: 10.1093/brain/122.5.871.
- [49] J. C. Hobart, A. Riazi, D. L. Lamping, R. Fitzpatrick, and A. J. Thompson, "Measuring the impact of MS on walking ability: The 12-Item MS Walking Scale (MSWS-12)," *Neurology*, vol. 60, no. 1, pp. 31–36, Jan. 2003, doi: 10.1212/WNL.60.1.31.
- [50] A. Holland, R. J. O'Connor, A. J. Thompson, E. D. Playford, and J. C. Hobart, "Talking the talk on walking the walk: A 12-item generic walking scale suitable for neurological conditions?," *J. Neurol.*, vol. 253, no. 12, pp. 1594–1602, Dec. 2006, doi: 10.1007/s00415-006-0272-2.
- [51] M. E. Tinetti, "Performance-oriented assessment of mobility problems in elderly patients," *J. Am. Geriatr. Soc.*, vol. 34, no. 2, pp. 119–126, Feb. 1986, doi: 10.1111/j.1532-5415.1986.tb05480.x.

- [52] O. Beauchet, B. Fantino, G. Allali, S. W. Muir, M. Montero-Odasso, and C. Annweiler, "Timed up and go test and risk of falls in older adults: A systematic review," *J. Nutr. Health Aging*, vol. 15, no. 10, pp. 933–938, Dec. 2011.
- [53] L. Wolfson, R. Whipple, P. Amerman, and J. N. Tobin, "Gait Assessment in the Elderly: A Gait Abnormality Rating Scale and Its Relation to Falls," *J. Gerontol.*, vol. 45, no. 1, pp. M12–M19, Jan. 1990, doi: 10.1093/geronj/45.1.M12.
- [54] A. V. Fried, J. Cwikel, H. Ring, and D. Galinsky, "ELGAM — Extra-laboratory gait assessment method: Identification of risk factors for falls among the elderly at home," *Int. Disabil. Stud.*, vol. 12, no. 4, pp. 161–164, Jan. 1990, doi: 10.3109/03790799009166609.
- [55] R. J. Mobbs *et al.*, "Gait metrics analysis utilizing single-point inertial measurement units: a systematic review," *mHealth*, vol. 8, p. 9, Jan. 2022, doi: 10.21037/mhealth-21-17.
- [56] D. Jarchi, J. Pope, T. K. M. Lee, L. Tamjidi, A. Mirzaei, and S. Sanei, "A Review on Accelerometry-Based Gait Analysis and Emerging Clinical Applications," *IEEE Rev. Biomed. Eng.*, vol. 11, pp. 177–194, 2018, doi: 10.1109/RBME.2018.2807182.
- [57] M. L. McGuire, "An Overview of Gait Analysis and Step Detection in Mobile Computing Devices," in *2012 Fourth International Conference on Intelligent Networking and Collaborative Systems*, Sep. 2012, pp. 648–651. doi: 10.1109/iNCoS.2012.110.
- [58] C. Frigo and P. Crenna, "Multichannel SEMG in clinical gait analysis: A review and state-of-the-art," *Clin. Biomech.*, vol. 24, no. 3, pp. 236–245, Mar. 2009, doi: 10.1016/j.clinbiomech.2008.07.012.

- [59] E. C. Wentink, V. G. H. Schut, E. C. Prinsen, E. C. Prinsen, J. S. Rietman, and P. H. Veltink, "Detection of the onset of gait initiation using kinematic sensors and EMG in transfemoral amputees," *Gait Posture*, vol. 39, no. 1, pp. 391–396, Jan. 2014, doi: 10.1016/j.gaitpost.2013.08.008.
- [60] F. Lorussi, W. Rocchia, E. P. Scilingo, A. Tognetti, and D. De Rossi, "Wearable, Redundant Fabric-Based Sensor Arrays for Reconstruction of Body Segment Posture," *IEEE Sens. J.*, vol. 4, pp. 807–818, Dec. 2004, doi: 10.1109/JSEN.2004.837498.
- [61] F. Amitrano *et al.*, "Design and Validation of an E-Textile-Based Wearable Sock for Remote Gait and Postural Assessment," *Sensors*, vol. 20, no. 22, p. E6691, Nov. 2020, doi: 10.3390/s20226691.
- [62] T. Hua, "Fabric Sensor based In-Shoe Plantar Pressure Measurement and Analysis System for Gait and Balance Analysis," Feb. 2010.
- [63] Yang, Chang-Ming, Tzu Lin Yang, Ching Wen Yang, and Hao Yang. "System and method for analyzing gait using fabric sensors." U.S. Patent 8,961,439, issued February 24, 2015.
- [64] R. Jia, A. P. Monk, D. W. Murray, S. J. Mellon, and J. A. Noble, "Greater trochanter tracking in ultrasound imaging during gait," in *2015 IEEE 12th International Symposium on Biomedical Imaging (ISBI)*, Apr. 2015, pp. 260–263.
- [65] S. Upadhyaya, W.-S. Lee, and C. Joslin, "Patient specific bone tracking using ultrasound for human movement analysis," in *2016 IEEE International Symposium on Medical Measurements and Applications (MeMeA)*, May 2016, pp. 1–5. doi: 10.1109/MeMeA.2016.7533738.

- [66] M. Pouliot, V. Joshi, J. Chauvin, R. Goubran, and F. Knoefel, "Differentiating assisted and unassisted bed exits using ultrasonic sensor," in *2012 IEEE International Instrumentation and Measurement Technology Conference Proceedings*, Graz, Austria, May 2012, pp. 1104–1108.
- [67] D. Alshamaa, A. Chkeir, R. Soubra, and F. Mourad-Chehade, "Measurement of Gait Speed using a Doppler Radar: Influence of Acceleration and Deceleration Zones," in *2019 IEEE Sensors Applications Symposium (SAS)*, Sophia Antipolis, France, Mar. 2019, pp. 1–5. doi: 10.1109/SAS.2019.8706123.
- [68] I. O. Joudeh *et al.*, "WiFi Channel State Information-Based Recognition of Sitting-Down and Standing-Up Activities," in *2019 IEEE International Symposium on Medical Measurements and Applications (MeMeA)*, Istanbul, Turkey, Jun. 2019, pp. 1–6.
- [69] I. O. Joudeh, A.-M. Cretu, R. B. Wallace, and R. A. Goubran, "Location Independence in Machine Learning Classification of Sitting-Down and Standing-Up Actions using Wi-Fi Sensors," in *2021 IEEE International Symposium on Medical Measurements and Applications (MeMeA)*, 2021, p. 6.
- [70] H. Fei, F. Xiao, J. Han, H. Huang, and L. Sun, "Multi-Variations Activity Based Gaits Recognition Using Commodity WiFi," *IEEE Trans. Veh. Technol.*, vol. 69, no. 2, pp. 2263–2273, Feb. 2020, doi: 10.1109/TVT.2019.2962803.
- [71] A. Kolb, E. Barth, R. Koch, and R. Larsen, "Time-of-Flight Sensors in Computer Graphics," *Proc Eurographics State Art Re*, vol. 2009, Nov. 2008.

- [72] M. O. Derawi, H. Ali, and F. A. Cheikh, *Gait recognition using time-of-flight sensor*. Gesellschaft für Informatik e.V., 2011. Accessed: Jun. 09, 2022. [Online]. Available: <http://dl.gi.de/handle/20.500.12116/18539>
- [73] W. Samson, A. Van Hamme, S. Sanchez, L. Cheze, S. Van Sint Jan, and V. Feipel, “Dynamic footprint analysis by time-of-flight camera,” *Comput. Methods Biomech. Biomed. Engin.*, vol. 15 Suppl 1, pp. 180–2, Sep. 2012, doi: 10.1080/10255842.2012.713629.
- [74] Xue, Zhaojun, Dong Ming, Wei Song, Baikun Wan, and Shijiu Jin. "Infrared gait recognition based on wavelet transform and support vector machine." *Pattern recognition* 43, no. 8 (2010): 2904-2910.
- [75] M. Nieto-Hidalgo, F. J. Ferrández-Pastor, R. J. Valdivieso-Sarabia, J. Mora-Pascual, and J. M. García-Chamizo, “A vision based proposal for classification of normal and abnormal gait using RGB camera,” *J. Biomed. Inform.*, vol. 63, pp. 82–89, Oct. 2016.
- [76] E. D’Antonio, J. Taborri, E. Palermo, S. Rossi, and F. Patane, “A markerless system for gait analysis based on OpenPose library,” in *2020 IEEE International Instrumentation and Measurement Technology Conference (I2MTC)*, Dubrovnik, Croatia, May 2020, pp. 1–6.
- [77] X. Gu, F. Deligianni, B. Lo, W. Chen, and G. Z. Yang, “Markerless gait analysis based on a single RGB camera,” in *2018 IEEE 15th International Conference on Wearable and Implantable Body Sensor Networks (BSN)*, Las Vegas, NV, Mar. 2018, pp. 42–45.

- [78] A. P. Rocha, H. M. P. Choupina, M. do C. Vilas-Boas, J. M. Fernandes, and J. P. S. Cunha, "System for automatic gait analysis based on a single RGB-D camera," *PLOS ONE*, vol. 13, no. 8, p. e0201728, Aug. 2018.
- [79] A. Dubois and F. Charpillet, "A gait analysis method based on a depth camera for fall prevention," in *2014 36th Annual International Conference of the IEEE Engineering in Medicine and Biology Society*, Chicago, IL, Aug. 2014, pp. 4515–4518.
- [80] W. Zhu, B. Anderson, S. Zhu, and Y. Wang, "A Computer Vision-Based System for Stride Length Estimation using a Mobile Phone Camera," in *Proceedings of the 18th International ACM SIGACCESS Conference on Computers and Accessibility*, Reno Nevada USA, Oct. 2016, pp. 121–130.
- [81] B. Wallace, T. N. E. Harake, R. Goubran, N. Valech, and F. Knoefel, "Preliminary results for measurement and classification of overnight wandering by dementia patient using multi-sensors," in *2018 IEEE International Instrumentation and Measurement Technology Conference (I2MTC)*, Houston, TX, May 2018, pp. 1–6.
- [82] L. Ault, R. Goubran, B. Wallace, H. Lowden, and F. Knoefel, "Smart Home Technology Solution for Nighttime Wandering in Persons with Dementia," *J. Rehabil. Assist. Technol. Eng.*, 2020.
- [83] J. Kaye *et al.*, "Methodology for Establishing a Community-Wide Life Laboratory for Capturing Unobtrusive and Continuous Remote Activity and Health Data," *JoVE J. Vis. Exp.*, no. 137, p. e56942, Jul. 2018.
- [84] A. Lorenz and R. Oppermann, "Mobile health monitoring for the elderly: Designing for diversity," *Pervasive Mob. Comput.*, vol. 5, no. 5, pp. 478–495, Oct. 2009.

- [85] “Collaborative Aging Research Using Technology (CART).”
<https://www.ohsu.edu/collaborative-aging-research-using-technology/cart-home>.
- [86] B. Samadi, M. Raison, C. Detrembleur, and L. Ballaz, “Real-time detection of reaction forces during gait on a ground equipped with a large force platform,” in *2014 Global Information Infrastructure and Networking Symposium (GIIS)*, Sep. 2014, pp. 1–3. doi: 10.1109/GIIS.2014.6934268.
- [87] Kutilek, Patrik, Ivan Vareka, Vaclav Krivanek, Petr Molnar, Zdenek Svoboda, Ondrej Nemecek, and Slavka Viteckova. "Gait Evaluation in Patients with Transtibial Prosthesis using Force Platforms." In *2018 18th International Conference on Mechatronics-Mechatronika (ME)*, pp. 1-4. IEEE, 2018.
- [88] F. Muheidat, H. W. Tyrer, M. Popescu, and M. Rantz, “Estimating walking speed, stride length, and stride time using a passive floor based electronic scavenging system,” in *2017 IEEE Sensors Applications Symposium (SAS)*, Glassboro, NJ, USA, 2017, pp. 1–5. doi: 10.1109/SAS.2017.7894112.
- [89] S. L. Bennett, R. Goubran, A. Arcelus, K. Rockwood, and F. Knoefel, “Pressure signal feature extraction for the differentiation of clinical mobility assessments,” in *2012 IEEE International Symposium on Medical Measurements and Applications Proceedings (MeMeA)*, May 2012, pp. 1–5.
- [90] T. L. Grant *et al.*, “Sit-To-Stand (STS) timing among older adults in their homes: Two measurement approaches,” *Gerontechnology*, vol. 12, no. 3, pp. 153–158, Jun. 2014.

- [91] Zhaofen Ren *et al.*, “Analyzing center of pressure progression during bed exits,” in *2014 36th Annual International Conference of the IEEE Engineering in Medicine and Biology Society*, Chicago, IL, Aug. 2014, pp. 1786–1789.
- [92] S. R. Simon, “Quantification of human motion: gait analysis-benefits and limitations to its application to clinical problems,” *J. Biomech.*, vol. 37, no. 12, pp. 1869–1880, Dec. 2004, doi: 10.1016/j.jbiomech.2004.02.047.
- [93] “Average Walking Speed: Pace, and Comparisons by Age and Sex.” <https://www.healthline.com/health/exercise-fitness/average-walking-speed#average-speed-by-sex>.
- [94] A. Batla, V. Phé, L. De Min, and J. N. Panicker, “Nocturia in Parkinson’s Disease: Why Does It Occur and How to Manage?,” *Mov. Disord. Clin. Pract.*, vol. 3, no. 5, pp. 443–451, Sep. 2016, doi: 10.1002/mdc3.12374.
- [95] T. L. Hayes, T. Riley, N. Mattek, M. Pavel, and J. A. Kaye, “Sleep Habits in Mild Cognitive Impairment,” *Alzheimer Dis. Assoc. Disord.*, vol. 28, no. 2, pp. 145–150, 2014, doi: 10.1097/WAD.0000000000000010.
- [96] “IEEE Standard for Low-Rate Wireless Networks,” *IEEE Std 802154-2020 Revis. IEEE Std 802154-2015*, pp. 1–800, Jul. 2020.